Effects of Nucleus Size and Position on the Response of the Lumbar Functional Spinal Unit L4-L5 to Complex Loading: Finite Element Analysis.

By

Fatemeh Fallahi Arezodar

A thesis submitted in partial fulfillment of the requirements for the degree of

Master of Science

In

Structural Engineering

Department of Civil and Environmental Engineering
University of Alberta

Abstract

The response of the lumbar spine to mechanical load, a major contributing factor in Low Back Pain (LBP), depends on the geometry of the spinal structures. As nucleus size and position vary among individuals, along the spine, and with aging, understanding the effects of inter-individual variation of the nucleus geometry on the mechanical behavior of spine is very important and can be very useful in LBP assessment. Numerical studies can provide insights on the effect of these variations on the mechanical response of the spine.

This study aimed to determine the variations of the size and position of the nucleus pulposus with respect to the disc in the lumbar level L4-L5 of 24 individuals using their MR images and to investigate the effects of these variations on the mechanical response of the Functional Spinal Unit (FSU) L4-L5 to various load combinations using the finite element (FE) method.

The MR images of the subjects were used to reconstruct the 3D geometries of the lumbar L4-L5 disc. The proportion of the nucleus cross-sectional area to the whole disc for all subjects was found between 31% and 57% and the nucleus centroid was located between 1.67 mm anteriorly and 3.26 mm posteriorly with respect to the disc center. Based on these results and the previous FE studies and histological findings, five FE models of the FSU L4-L5 with distinct sizes and positions of the nucleus were developed. The models were subjected to 10Nm moments in all anatomic planes with or without a 500N follower load (FL) as well as moment with direction varying gradually by about 15^{o} between anatomical planes combined with FL.

The intradiscal pressure (IDP) in nucleus pulposus, the annular fibers strain, and the intervertebral rotation (IVR) predicted by the FE models were compared. The IDP was significantly influenced

by the variations in size and position of the nucleus under pure moment. Adding FL attenuated these effects on IDP.

The maximum strain location and magnitude in the annular fibers were sensitive to the position and size of the nucleus. Maximum of the fibers strain and nucleus size were directly proportional under FL and flexion as well as FL and extension. However, by shifting the nucleus position toward the posterior side of the disc, the maximum fibers strain increased under FL and flexion while a drop was obtained under FL and extension.

Result showed that the nucleus size and position had slight effects on IVR. The FSU with the large nucleus compared to one with the small nucleus as well as the FSU with the anterior position of the nucleus compared to one with the posterior position of the nucleus demonstrated stiffer behaviour.

This study demonstrated that the geometrical variations of the nucleus size and position influence the mechanical response of the L4-L5 FSU but the significance of these effects was dependent on the loading scenario. It is speculated that including the fluid phase in disc modeling, analyzing the whole lumbar spine, and applying *in-vivo* loading would reveal more remarkable effects.

Preface

This thesis is an original work by Fatemeh Fallahi Arezodar. The research project, of which this thesis is a part, received research ethics approval from the University of Alberta Health Research Ethics Board - Health Panel, Project Name "Effects of Variation in Individual Patient Anatomy on Load-Sharing in Lumbar Spine: Finite Element Analyses Using Personalized 3D Models.", No. Pro00037684, February 14, 2013.

Chapter 5 of this thesis has been submitted to the Journal of Biomechanics as F. Fallahi Arezodar, S. Naserkhaki, K., Duke, S. Adeeb, M. El-Rich, "Effects of Nucleus Size and Position on the Response of the Lumbar Functional Spinal Unit L4-L5 to Complex Loading: Finite Element Analysis". I was responsible for the analysis as well as the manuscript composition. Dr. Naserkhaki provided the geometry of the bony structure and reviewed the manuscript. Dr. Duke provided the support required for the statistical analysis and reviewed the manuscript. Dr. El-Rich and Dr. Adeeb were the supervisory authors and were involved with concept formation, FE analyses and manuscript composition. Also, Dr. Jaremko provided the CT scans and MR images.

Dedication

To my beloved husband Hamed, my wonderful parents Susan and Alireza, my amazing son Parsa, my dear siblings Hossein, Zeinab and Mohammad Mahdi, and to my kind in-laws Masoomeh and Mohammad.

Acknowledgments

I would like to express my sincere gratitude to Dr. Marwan El-Rich, my supervisor, for his warm greetings, supportive attitude, guidance and immense knowledge. He patiently provided the vision, encouragement and valuable input through my research at University of Alberta. I also need to thank him for the trust and confidence that he has shown in me, which helped me to work to the best of my ability. Undoubtedly, without his constant help and supervision, this dissertation would not have been possible.

I would like to express my deepest appreciation to my co-supervisor Dr. Samer Adeeb for his nice attitude, valuable contributions and providing me with constructive comments. He taught me finite element which was a great help in my project. For that, I am truly grateful and thank him very much.

I would like to thank Dr. Kajsa Duke for providing her valuable advice in the statistical analysis and for reviewing my thesis. Her precious comments and advices on my research are greatly appreciated.

I also thank Dr. Jacob L. Jaremko for providing CT scans and MR images that greatly assisted the measurements of disc geometry and FE modeling.

Special thanks must be made to my friends and colleagues at the Structural Engineering group at University of Alberta for their help and support. I extend my appreciation to Dr. Sadegh Naserkhaki for all his time and his valuable help.

I wish to thank my family for all of their support. I would like to express my deep sincere gratitude to my parents for their support and for giving me the very best that they could. Without their continuous support and encouragement, I would never have been able to achieve my goals. A special thanks to my husband for all his love, support, and understanding through my research. Words cannot describe how blessed I am to have him in my life. He has selflessly given more to me than I ever could have asked for.

I gratefully acknowledge the financial support I received from my supervisor, Faculty of Graduate Study and Research (FGSR), and Graduate Student Association (GSA). Additionally, the Natural Sciences and Engineering Research Council of Canada (NSERC) provided partial funding for this project.

Table of Contents

List of Tables

List of Figures

Chapter 1: Introduction

1.1. Overview

The spine is a mechanical structure which serves as a central support to transfer the weight of the body to the pelvis; it allows physiological movements, and protects the spinal cord from potential damage (White III and Panjabi, 1978). These functions are achieved thanks to the synergy between the spinal structures. Malfunction of any components of the spine could affect other components' contribution in load-bearing and ultimately cause injury and pain.

Low back pain (LBP) is one of the most common chronic pains affecting activities of daily living and work performance and it is prevalent among 70% of general population (Schmidt at al., 2007b; Waters et al., 1993). Mechanical load is one of various potential causes of LBP (McGill, 2015). Many studies were performed to investigate the mechanical behaviour of the spine and the spinal load-sharing which describe the role of each spinal component in resisting loads (Naserkhaki et al., 2016a, 2016b; El-Rich et al., 2009; Jacobs et al. 2014; Noilley et al., 2007; Schmidt at al., 2007a, 2007b; Panjabi et al., 1994; Shirazi-Adl et al.,1986,1984).

In previous studies, a strong relationship between intervertebral disc morphology and an increased risk of low back pain has been reported (Hickey & Hukins, 1980; Natarajan & Andersson, 1999). Thus, understanding the effect of inter-individual disc geometry variation on spinal response is very important for determination of the causes of LBP and design of intervertebral disc implants. As the intervertebral disc's geometric parameters govern its biomechanical properties (Natarajan & Andersson, 1999), geometry variations of the intervertebral disc including size and position of the nucleus might affect the mechanical behaviour of the spine (Naserkhaki et al., 2016a, 2016b; Schmidt et al., 2007b; Noilley et al., 2007; Natarajan & Andersson., 1999).

Some *in-vitro* and numerical studies compared the lumbar disc height and cross-sectional area among people and among disc levels of the same spine and studied the effects of these variations on the mechanical response of the disc (Meijer et al., 2011; Noilley et al., 2007; Natarajan & Andersson., 1999; Pooni et al., 1986; Nachemson et al., 1979). However, to the best of our knowledge, there has been no attempt to investigate the influence of the size and position of the nucleus on the mechanical response of the spine under various load combinations.

Due to inherent inter-individual variability, experimental (*in-vitro* and *in-vivo*) studies could not clearly identify the effect of geometry variations on the spinal segment behavior (Schmidt et al., 2007b; Noilley et al., 2007; Nachemson et al., 1979). Numerical studies can, however, be very

helpful to study the effects of varying one parameter on the other ones which will help interpreting the experimental result (Schmidt et al., 2007b; Noilley et al., 2007).

In the current study, the size of the nucleus and the position of the nucleus centroid with respect to the disc center at the level L4-L5 were determined in 24 individuals using their MRI data. Then, five 3D nonlinear FE models of the FSU L4-L5 with distinct sizes and positions of the nucleus were created. One of these models; the one with nucleus cross-sectional area of 44% of the total disc and centroid located in the disc center was validated in previous study (Naserkhaki et al., 2017b). These models were subjected to various load combinations. The responses of the segments to mechanical load in terms of stiffness and internal loads were compared.

1.2. Hypothesis

The size and position of the nucleus with respect to the disc vary among individuals, along the same spine and with ageing. As the response and internal loads of any structure such as a spinal segment is highly related to its shape and geometry, it is hypothesized that the variation in geometry and position of the nucleus affects the behaviour of the spinal functional unit (FSU) under mechanical load and the effects vary with the loading scenario.

1.3. Objectives

The current study aimed to:

1. Measure the position and size of L4-L5 nucleus of 24 individuals using their MRI data
2. Determine the effects of size and position of the nucleus on the response of the FSU L4-L5 to various load combinations using FE method

1.4. Scope and limitations

To limit the geometrical parameters, the current research used five FE models having similar geometry of the ligaments and the vertebrae L4 and L5. This geometry was used in the FE model developed and validated by Naserkhaki et al. (2016a). Muscles were not included in the FE models. The loading scenario used is an approximation of the realistic (*in-vivo*) load which includes the body weight, muscle forces and varies with the spine posture (Dreischarf et al., 2016; Naserkhaki et al., 2016a; Rohlmann et al., 2009a, 2009b; Arjmand & Shirazi-Adl, 2006; El-Rich et al., 2004). A compressive follower load (FL) whose line of action passes through the center of each vertebra

was used to simulate muscle force (Naserkhaki et al., 2016b; 2017b; Patwardhan et al., 1999). However, due to spinal segment asymmetry, the FL did not pass through the exact center of disc which produced a slight rotation in addition to the compression. The material properties of the spinal components were the same in all FE models except the annular fibers. Moreover, as the overall volume of the annular fibers should be kept 16% of the annulus volume (Naserkhaki et al., 2016b, 2017b; Shirazi-Adl et al., 1984), their material properties were modified according to the nucleus size. The fluid phase in the disc and the variation of other geometric parameters such as disc height or cross-sectional area along the disc height were not considered in this study.

1.5. Outline of the thesis

Chapter 1

The overall overview of the subject is discussed. The Hypothesis and objectives are defined and the scope and limitations of this study are clarified.

Chapter 2

A literature review on the spine, lumbar functional spinal unit, and the intervertebral disc geometry in numerical and experimental studies is provided.

Chapter 3

The method used to recreate the 3D models of the disc and nucleus from MRI data and the method of measuring the cross-sectional area and position of the nucleus is explained. The results of the measurements are presented.

Chapter 4

A detailed description of the step-by-step procedure used to create the FE models with different sizes and positions of the nucleus is provided. The assumptions and limitations of the material properties and loading scenarios used are highlighted.

Chapter 5

Effects of the nucleus size and position on the response of the FSU L4-L5 to various load combinations are investigated and discussed. This chapter has been submitted as a research manuscript to the journal of Biomechanics.

Chapter 6

Findings of the current research are summarized. Conclusions and recommendation are provided.

References

Arjmand, N., & Shirazi-Adl, A. (2006). Model and in vivo studies on human trunk load partitioning and stability in isometric forward flexions. Journal of biomechanics, 39(3), 510-521.

Campana, S., Guise, J. A., Rillardon, L., Mitton, D., & Skalli, W. (2007). Lumbar intervertebral disc mobility: Effect of disc degradation and of geometry. European Journal of Orthopaedic Surgery & Traumatology, 17(6), 533. doi:10.1007/s00590-007-0243-z

Dreischarf, M., Shirazi-Adl, A., Arjmand, N., Rohlmann, A., & Schmidt, H. (2016). Estimation of loads on human lumbar spine: a review of in vivo and computational model studies. Journal of biomechanics, 49(6), 833-845.

El-Rich, M., Arnoux, P. J., Wagnac, E., Brunet, C., & Aubin, C. E. (2009). Finite element investigation of the loading rate effect on the spinal load-sharing changes under impact conditions. Journal of biomechanics, 42(9), 1252-1262.

El-Rich, M., Shirazi-Adl, A., & Arjmand, N. (2004). Muscle activity, internal loads, and stability of the human spine in standing postures: combined model and in vivo studies. Spine, 29(23), 2633-2642.

Hickey, D.S., & Hukins, D.W.L (1980). Relation between the structure of the annulus fibrosus and the function and failure of the intervertebral disc. Spine, 5(2), 106-116.

Jacobs, N. T., Cortes, D. H., Peloquin, J. M., Vresilovic, E. J., & Elliott, D. M. (2014). Validation and application of an intervertebral disc finite element model utilizing independently constructed tissue-level constitutive formulations that are nonlinear, anisotropic, and time-dependent. Journal of biomechanics, 47(11), 2540-2546.

McGill, S. M. (2015). Low Back Disorders, 3E. Human Kinetics.

Nachemson, A. L., Schultz, A. B., & Berkson, M. H. (1979). Mechanical properties of human lumbar spine motion segments: Influences of age, sex, disc level, and degeneration. Spine, 4(1), 1-8.

Naserkhaki, S., Arjmand, N., Shirazi-Adl, A., Farahmand, F., & El-Rich, M. (2017b). Effects of eight different ligament property datasets on biomechanics of a lumbar L4-L5 finite element model. Journal of Biomechanics.

Naserkhaki, S., Jaremko, J. L., & El-Rich, M. (2016a). Effects of inter-individual lumbar spine geometry variation on load-sharing: Geometrically personalized finite element study. Journal of Biomechanics, 49(13), 2909-2917.

Naserkhaki, S., Jaremko, J. L., Adeeb, S., & El-Rich, M. (2016b). On the load-sharing along the ligamentous lumbosacral spine in flexed and extended postures: Finite element study. Journal of biomechanics, 49(6), 974-982.

Natarajan, R. N., & Andersson, G. B. (1999). The influence of lumbar disc height and cross-sectional area on the mechanical response of the disc to physiologic loading. Spine, 24(18), 1873.

Noailly, J., Wilke, H. J., Planell, J. A., & Lacroix, D. (2007). How does the geometry affect the internal biomechanics of a lumbar spine bi-segment finite element model? Consequences on the validation process. Journal of biomechanics, 40(11), 2414-2425.

Panjabi, M.M., Oxland, TR., Yamamoto I., & Crisco, JJ. (1994). Mechanical behavior of the human lumbar and lumbosacral spine as shown by three-dimensional load-displacement curves. The Journal of Bone & Joint Surgery, 76(3), 413-424. doi:10.2106/00004623-199403000-00012

Patwardhan, A. G., Havey, R. M., Meade, K. P., Lee, B., & Dunlap, B. (1999). A Follower Load Increases the Load-Carrying Capacity of the Lumbar Spine in Compression. Spine, 24(10), 1003-1009.

Pooni, J. S., Hukins, D. W., Harris, P. F., Hilton, R. C., & Davies, K. E. (1986). Comparison of the structure of human intervertebral discs in the cervical, thoracic and lumbar regions of the spine. Surgical and Radiologic Anatomy: SRA, 8(3), 175-182. doi:10.1007/BF02427846

Rohlmann, A., Zander, T., Rao, M., & Bergmann, G. (2009a). Realistic loading conditions for upper body bending. Journal of Biomechanics, 42(7), 884-890.

Rohlmann, A., Zander, T., Rao, M., & Bergmann, G. (2009b). Applying a follower load delivers realistic results for simulating standing. Journal of biomechanics, 42(10), 1520-1526.

Schmidt, H., Kettler, A., Rohlmann, A., Claes, L., & Wilke, H. J. (2007a). The risk of disc prolapses with complex loading in different degrees of disc degeneration–a finite element analysis. Clinical Biomechanics, 22(9), 988-998.

Schmidt, H., Kettler, A., Heuer, F., Simon, U., Claes, L., & Wilke, H. J. (2007b). Intradiscal pressure, shear strain, and fiber strain in the intervertebral disc under combined loading. Spine, 32(7), 748-755

Shirazi-Adl, A. A. A. S. S., Ahmed, A. M., & Shrivastava, S. C. (1986). Mechanical response of a lumbar motion segment in axial torque alone and combined with compression. Spine, 11(9), 914-927.

Shirazi-adl, S. A., Shrivastava, S. C., & Ahmed, A. M. (1984). Stress Analysis of the Lumbar Disc-Body Unit in Compression A Three-Dimensional Nonlinear Finite Element Study. Spine, 9(2), 120-134.

Waters, T. R., Putz-Anderson, V., Garg, A., & Fine, L. J. (1993). Revised NIOSH equation for the design and evaluation of manual lifting tasks. Ergonomics, 36(7), 749-776.

White III, A.A., Panjabi, M.M. (1990). Clinical Biomechanics of the Spine, second ed. Lippincott Williams & Wilkins.

Chapter 2: Background

2.1. Human spine anatomy

Spine or the back bone, also called vertebral column, is made of 33 or 34 individual bones named vertebrae. The vertebral column provides the main support for the head, arms and trunk, allowing flexible movement of the body such as bending and twisting, while protecting the spinal cord from potentially damaging forces or motions (Watkins, 2010; White III & Panjabi, 1990)

The vertebrae are divided to five regions: cervical, thoracic, lumbar, sacral and coccygeal (Fig. 2.1). The cervical spine, located in the neck region, consists of 7 vertebrae. The thoracic region, located in the chest region, includes 12 vertebrae. The lumbosacral region of the spine or lumbar spine, also called lower back, is composed of 5 vertebrae in total. Below the lumbar spine is the sacral region which is made of 5 sacral vertebrae fused together. The very bottom part of spine is called the coccygeal region consisting of 4 or 5 vertebrae, depending on an individual's development. The vertebrae of this region fuse together to make the coccyx or tailbone. Each vertebra (except the first two cervical vertebrae) is composed of three bony elements called vertebral body, endplates and posterior elements. The posterior elements consist of the lamina, pedicles, articular, spinous and transverse processes. The adjacent vertebrae are connected by a fibrocartilaginous disc called an intervertebral disc (Watkins, 2010).

2.2. Lumbar spine anatomy

The lumbar vertebrae are labeled by the first letter of lumbar region and according to their position in the intact column as L1, L2, L3, L4, and L5 (Bogduk, 2005). The vertebrae of the lumbosacral spine are bigger and stronger than the vertebrae in the cervical and thoracic regions (Benzel, 2011). The weight of the upper body is mainly supported by the lumbar spine (Cholewicki & McGill, 1996). The orientation of the fact joints of the lumbar vertebrae cause the axial rotation of lumbar vertebrae to be limited. However, much greater range of motion in other directions is related to the relatively thick intervertebral discs in the lumbar region (Watkins, 2010). Each FSU of lumbar vertebrae are supported by 7 major ligaments: the anterior longitudinal (ALL), posterior longitudinal (PLL), capsular (CL), intertransverse (ITL), supraspinous (SSL), interspinous ligaments (ISL), and ligamentum flavum (LF) (Breau et al., 1991).

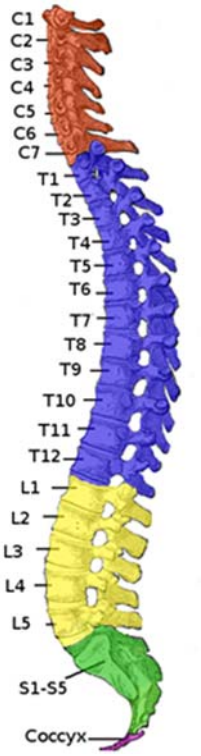

Fig. 2.1. Vertebral column (Adopted from https://commons.wikimedia.org/wiki/File:Gray_111_-_Vertebral_column-coloured_labels.png) (Public Domain)

2.3. Motion segment

A smallest functional unit of spine showing the biomechanical characteristics similar to the entire spine is called a motion segment or functional spinal unit (FSU). Two adjacent vertebrae, an intervertebral disc, facet joints, and ligaments are the component of a functional spinal unit (Sharma & Rodriguez,1995) (Fig. 2.2). Stability of the functional unit is mainly obtained by ligaments, facet joints and intervertebral disc. These three stabilizers work together to provide the stability of the motion segment. However, their roles can alter according to the type of loading (Sharma & Rodriguez,1995).

During various daily activities, the lumbar FSU is subjected to the various complex loading cases (Shirazi-Adl et al., 1986). Excessive loading can damage the FSU and cause pain (McGill, 2015). A clinical study of low back pain revealed that the functional spinal unit level L4-L5 was the most painful segment (Beneck et al., 2005). Also, this segment is described as the more common sites of pathology in clinical literature (Beneck et al., 2005; Bigos et al., 1994; Kirkaldy-Willis & Farfan., 1982; Soini et al., 1991).

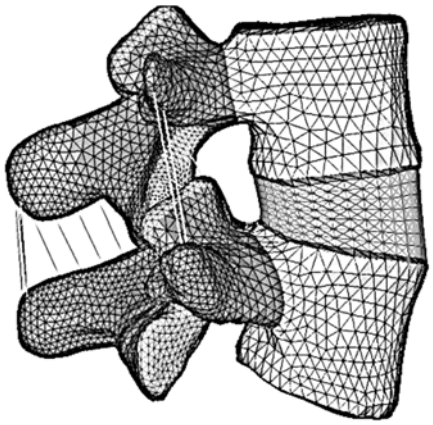

Fig. 2.2. L4-L5 motion segment or functional spinal unit

2.4. Intervertebral disc

The intervertebral disc, which is a complex structure, has many functions. The disc allows movement between two adjacent vertebrae, absorbing and resisting shocks, while transmitting load along spine (Schmidt et al., 2013; Lundon & Bolton, 2001; White III & Panjabi, 1990). The intervertebral disc constitutes around 15-20% of the entire length of the spine (Shapiro & Risbud, 2014).

The intervertebral disc consists of 3 distinct parts: (1) the nucleus pulposus (NP), a central gelatinous core; (2) the annulus fibrosus (AF) described as a surrounding ring; and (3) the cartilaginous endplates (Fig. 2.3)

The nucleus pulposus is a hydrated, soft deformable central region of the intervertebral disc. It is made up of proteoglycan gel, water, and a very loose network of collagen (Adams, 2015; White III & Panjabi, 1990). The water content in nucleus is about 70% to 85% (Shapiro & Risbud, 2014). The high level of water in nucleus makes the nucleus pulposus acts like a pressurized fluid exhibiting a hydrostatic pressure in compression (Adams, 2015). The most important function of the nucleus pulposus is to support applied load with distributing a force to all direction within each intervertebral disc (Shapiro & Risbud, 2014; Lundon & Bolton, 2001).

The annulus fibrosus, which is the exterior part of the intervertebral disc, is composed of multilayer concentric lamellae with aligned annular fibers networks within each layer of lamella (Raj, 2008). The stiffness of annular fibers increases from inner layer to the outer layer. The overall volume of the annular fibers is about 16% of the total volume of annulus (Shirazi-Adl et al, 1984). The

annular fibers are oriented at an angle close to ±35° to the horizontal plane in crosswise pattern (Raj, 2008; El-Rich et al., 2007; Natarajan & Andersson, 1999; White III & Panjabi, 1990). The main function of the annulus fibrosus is to provide a lateral confinement for the highly pressurized nucleus, while resisting compressive load (Adams, 2015; Shapiro & Risbud, 2014)

The cartilage endplate, which is also called vertebral endplate, is made up of hyaline cartilage separating the disc and adjacent vertebral bodies (Adams, 2015; Shapiro & Risbud, 2014).

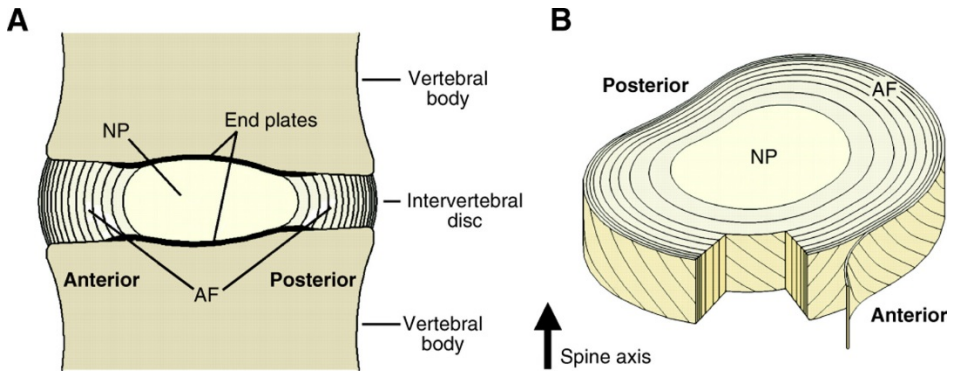

Fig. 2.3. Schematic representations of the adult intervertebral disc. (a) mid-sagittal cross-section showing anatomical regions, (b) three-dimensional view illustrating AF lamellar structure (Adopted from Smith et al., 2011) (Figure is licensed under CC by 4.0).

2.5. Geometry variation of intervertebral disc

The geometry of the intervertebral disc varies among individuals, along the same spine, and with aging (Pooni et al., 1986; Meijer et al., 2011; O'Connell et al., 2007). Some of these geometrical changes can affect possible mechanisms of failure of the spinal structures (Pooni et al., 1986).

The cervical discs have an elliptical cross-section (Fig. 2.4a). However, the discs of the thoracic spine tend to have a more rounded shape (Fig. 2.4b). The cross-section of the lumbar intervertebral discs is approximately elliptical that it is flattened in the posterior side (Fig. 2.4c) (Lundon & Bolton, 2001; Pooni et al., 1986). Due to the circular cross-section of the discs in thoracic spine, these discs experience a uniform distribution of the stress around the annulus in torsion and compression; however, they could be quickly damaged in flexion as the stress is mainly transmitted to the posterior annular fibers. In contrast, the possibility of the damage in the discs with elliptical

cross-section (especially flattened and re-entrant discs) is less in flexion compared to circular shape. On the other hand, these shapes are expected to be weaker in torsion. The discs of lumbar spine particularly L4-L5 and L5-S1 are even more quickly damaged by torsion due to the concentrated stress at the points of maximum curvature. The posterior protrusions which could be the dominant cause of back pain can be caused by torsion (Hickey & Hukins, 1980).

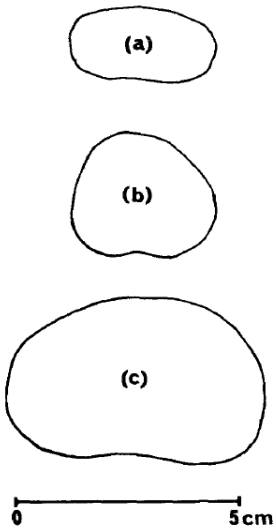

Fig. 2.4**.** Cross-sectional shapes of: (a) C7-T1, (b) T7-8, and (c) L4-5 disc (Adopted from Pooni et al., 1986) (Figure is used with permission of Springer).

The cross-sectional area of the intervertebral disc increases from the cervical region to the lumbar region (Pooni et al., 1986). Also, the area of lumbar disc varies among individuals and with age (Natarajan & Andersson, 1999). According to previous studies, the size of the disc area increases with age (Koeller et al., 1986; Amonoo-Kuofi, 1991). Also, according to an *in-vitro* human cadaveric study, the transverse cross-sectional area of the lumbar disc is smaller in women than men and as a result female segments experience considerably larger increase in intradiscal pressure (IDP) than male in response to compressive load (Nachemson et al., 1979). Natarajan and Andersson (1999) found that the stiffness of the FSUs and cross-sectional area of the lumbar discs were directly proportional in all loading modes. However, IDP increased when the cross-sectional area of the disc was decreased. They also concluded that a disc with a smaller cross-sectional area is expected to be more vulnerable to instability compared to a disc with greater cross-sectional area.

The height of the disc varies among people, between male and female, with age and, within disc itself as a function of loading (Natarajan & Andersson, 1999). The height of the disc in the thoracic region is smaller than in another regions of the spine (Middleditch & Oliver, 2005; Pooni et al., 1986). In contrast, the disc thickness is found to be the greatest in the lumbar region (Pooni et al., 1986). The stiffness of the disc is expected to drop when the disc height increases (Middleditch & Oliver, 2005; Natarajan & Andersson, 1999; Pooni et al., 1986). However, the flexibility of thoracic and lumbar discs is almost the same in flexion, extension, and lateral bending due to the larger cross-sectional area of the lumbar disc (Middleditch & Oliver, 2005). Adams et al. (1990) found that the height of the disc decreases in compression and flexion because of creep loading which increases stiffness of the disc in these directions (Natarajan & Andersson, 1999). In another study investigating the influence of interpersonal geometrical variation on FSU stiffness, Meijer et al. (2011) reported that variation of the disc height had the largest influence on the stiffness of the FSU compared to the effects of other geometrical variation. In all loading cases except extension, the highest IDP was obtained in the disc with the least height (Natarajan & Andersson, 1999).

In addition to height and cross-sectional area of the disc, position and size of the nucleus with respect to the disc also vary among individuals, along the same spine and with ageing (Pooni et al., 1986; Meijer et al., 2011, O'Connell et al., 2007). The size of the lumbar nucleus is the largest compared to those in other regions of the spine (White III & Panjabi, 1990). A 3D model of lumbar spine was reconstructed from CT scan data of a 65-year-old male subject by Breau et al. (1991). According to the reported measurements of the reconstructed lumbar discs, the cross-sectional area of the nucleus in midplane was about 44% of the disc cross-sectional area. In a histological study of L4-L5 intervertebral disc, Schmidt at al. (2006) found that the nucleus occupies approximately 44% of the disc area and its center is located 3.5 mm posteriorly from the disc center. Other study by Shirazi et al. (1984) reported that proportion of cross-sectional area of the nucleus pulposus to the whole disc varies between 30-60%. White III and Panjabi (1990) noted that the lumbar nucleus occupies 30-50% of the total cross-sectional area of the disc and with a center located in a third of the distance between center of the disc and posterior side of the disc. In another study on three L4-L5 discs obtained from tissue bank, the nucleus cross-sectional area was found about 28% of the area of the whole disc and the center of the nucleus was located 1.17 mm posteriorly (O'Connell et al., 2007). Meijer et al. (2011) found negligible effect on the stiffness of the lumbar FSU under

pure moment after changing the size of the nucleus between 30% and 50%. Fig. 2.5 shows the L4-L5 disc with different size and position of nucleus.

Despite previous findings on effects of variation of disc geometry on mechanical response of functional spinal unit or entire spine, there is still lack of knowledge on effects of nucleus size and position on mechanical response of spine. As the variability is inherent in experimental (*in-vitro* or *in-vivo*) studies, the effect of geometry variations such as nucleus size and position on the spinal segment could not clearly be identified (Schmidt et al., 2007b; Noilley et al., 2007; Nachemson et al., 1979). On the other hand, numerical and FE models allow parametric studies of inter-individual geometry variation effects on the spine behaviour which would help interpreting the experimental result (Schmidt et al., 2007b; Noilley et al., 2007).

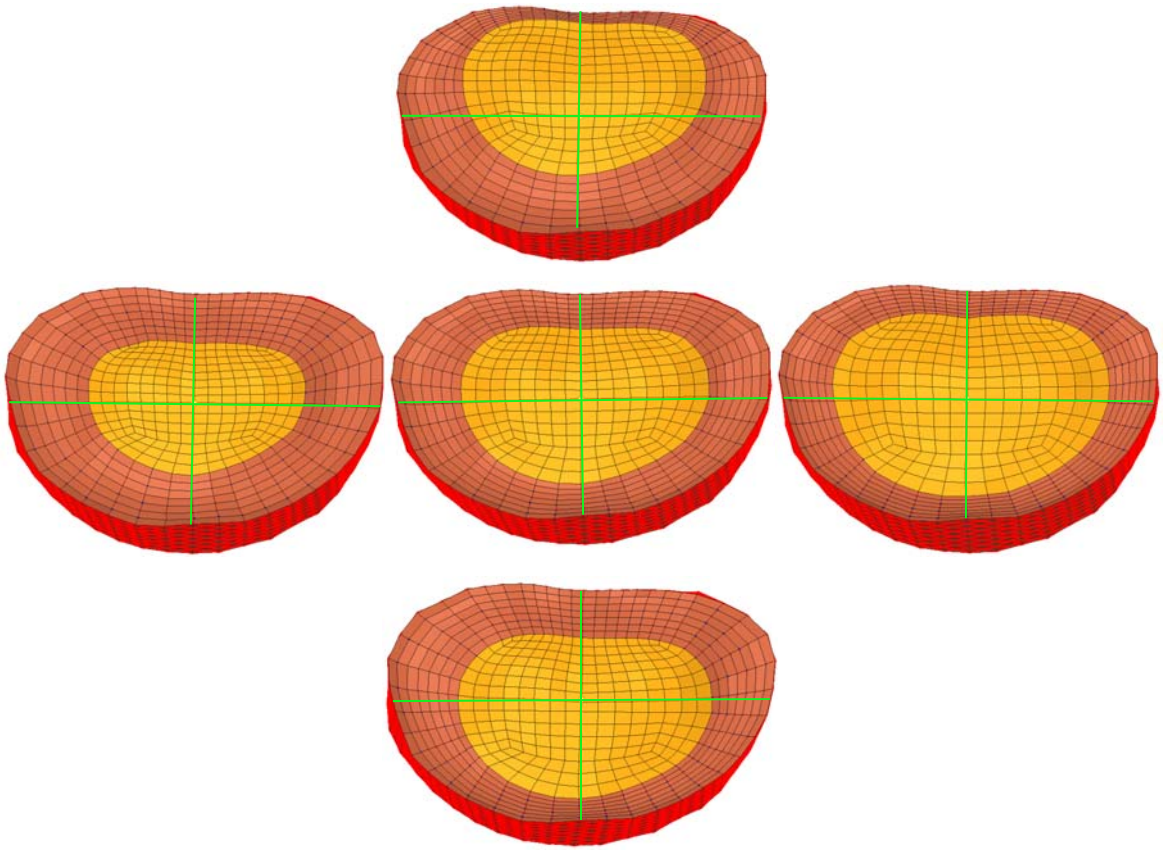

Fig. 2.5**.** Different sizes and positions of L4-L5 nucleus in intervertebral disc

References

Adams, M. A. (2015). Intervertebral Disc Tissues. In Mechanical Properties of Aging Soft Tissues (pp. 7-35). Springer International Publishing.

Adams, M. A., Dolan, P., Hutton, W. C., & Porter, R. W. (1990). Diurnal changes in spinal mechanics and their clinical significance. Bone & Joint Journal, 72(2), 266-270.

Amonoo-Kuofi, H. S. (1991). Morphometric changes in the heights and anteroposterior diameters of the lumbar intervertebral discs with age. Journal of anatomy, 175, 159.

Beneck, G. J., Kulig, K., Landel, R. F., & Powers, C. M. (2005). The relationship between lumbar segmental motion and pain response produced by a posterior-to-anterior force in persons with nonspecific low back pain. Journal of Orthopaedic & Sports Physical Therapy, 35(4), 203-209.

Benzel, E. C. (Ed.). (2011). Biomechanics of spine stabilization. Thieme.

Bigos, S., Bowyer, O., Braen, G., Brown, K., Deyo, R., Haldeman, S., Hart, J.L., Johnson, E.W., Keller, R., Kido, D. & Liang, M. H. (1994). Acute lower back problems in adults. Rockville, MD: Agency for Health Care Policy and Research.

Bogduk, N. (2005). Clinical anatomy of the lumbar spine and sacrum. Elsevier Health Sciences.

Breau, C., Shirazi-Adl, A., & De Guise, J. (1991). Reconstruction of a human ligamentous lumbar spine using CT images—a three-dimensional finite element mesh generation. Annals of biomedical engineering, 19(3), 291-302.

Cholewicki, J., & McGill, S. M. (1996). Mechanical stability of the in vivo lumbar spine: implications for injury and chronic low back pain. Clinical biomechanics, 11(1), 1-15.

Hickey, D.S., & Hukins, D.W.L (1980). Relation between the structure of the annulus fibrosus and the function and failure of the intervertebral disc. Spine, 5(2), 106-116.

Kirkaldy-Willis, W. H., & Farfan, H. F. (1982). Instability of the lumbar spine. Clinical orthopaedics and related research, 165, 110-123.

Koeller, W., Muehlhaus, S., Meier, W., & Hartmann, F. (1986). Biomechanical properties of human intervertebral discs subjected to axial dynamic compression—influence of age and degeneration. Journal of Biomechanics, 19(10), 807-816.

Lundon, K., & Bolton, K. (2001). Structure and function of the lumbar intervertebral disk in health, aging, and pathologic conditions. Journal of Orthopaedic & Sports Physical Therapy, 31(6), 291-306.

McGill, S. M. (2015). Low Back Disorders, 3E. Human Kinetics.

Meijer, G. J., Homminga, J., Veldhuizen, A. G., & Verkerke, G. J. (2011). Influence of interpersonal geometrical variation on spinal motion segment stiffness: implications for patient-specific modeling. Spine, 36(14), E929-E935.

Middleditch, A., & Oliver, J. (2005). Functional anatomy of the spine. Elsevier Health Sciences.

Nachemson, A. L., Schultz, A. B., & Berkson, M. H. (1979). Mechanical properties of human lumbar spine motion segments: Influences of age, sex, disc level, and degeneration. Spine, 4(1), 1-8.

Natarajan, R. N., & Andersson, G. B. (1999). The influence of lumbar disc height and cross-sectional area on the mechanical response of the disc to physiologic loading. Spine, 24(18), 1873.

Noailly, J., Wilke, H. J., Planell, J. A., & Lacroix, D. (2007). How does the geometry affect the internal biomechanics of a lumbar spine bi-segment finite element model? Consequences on the validation process. Journal of biomechanics, 40(11), 2414-2425.

O'Connell, G. D., Vresilovic, E. J., & Elliott, D. M. (2007). Comparison of animals used in disc research to human lumbar disc geometry. Spine, 32(3), 328-333.

Pooni, J. S., Hukins, D. W., Harris, P. F., Hilton, R. C., & Davies, K. E. (1986). Comparison of the structure of human intervertebral discs in the cervical, thoracic and lumbar regions of the spine. Surgical and Radiologic Anatomy: SRA, 8(3), 175-182. doi:10.1007/BF02427846

Raj, P. P. (2008). Intervertebral Disc: Anatomy-Physiology-Pathophysiology-Treatment. Pain Practice, 8(1), 18-44.

Schmidt, H., Galbusera, F., Rohlmann, A., & Shirazi-Adl, A. (2013). What have we learned from finite element model studies of lumbar intervertebral discs in the past four decades?. Journal of biomechanics, 46(14), 2342-2355.

Schmidt, H., Kettler, A., Heuer, F., Simon, U., Claes, L., & Wilke, H. J. (2007b). Intradiscal pressure, shear strain, and fiber strain in the intervertebral disc under combined loading. Spine, 32(7), 748-755

Schmidt, H., Heuer, F., Simon, U., Kettler, A., Rohlmann, A., Claes, L., & Wilke, H. J. (2006). Application of a new calibration method for a three-dimensional finite element model of a human lumbar annulus fibrosus. Clinical Biomechanics, 21(4), 337-344.

Shapiro, I., & Risbud, M. (2014). The intervertebral disc: Molecular and structural studies of the disc in health and disease

Sharma, M., Langrana, N. A., & Rodriguez, J. (1995). Role of ligaments and facets in lumbar spinal stability. Spine, 20(8), 887-900.

Shirazi-Adl, A. A. A. S. S., Ahmed, A. M., & Shrivastava, S. C. (1986). Mechanical response of a lumbar motion segment in axial torque alone and combined with compression. Spine, 11(9), 914-927.

Shirazi-adl, S. A., Shrivastava, S. C., & Ahmed, A. M. (1984). Stress Analysis of the Lumbar Disc-Body Unit in Compression A Three-Dimensional Nonlinear Finite Element Study. Spine, 9(2), 120-134.

Smith, L. J., Nerurkar, N. L., Choi, K. S., Harfe, B. D., & Elliott, D. M. (2011). Degeneration and regeneration of the intervertebral disc: lessons from development. Disease models & mechanisms, 4(1), 31-41.

Soini, J., Antti-Poika, I., Tallroth, K., Konttinen, Y. T., Honkanen, V., & Santavirta, S. (1991). Disc degeneration and angular movement of the lumbar spine: comparative study using plain and flexion-extension radiography and discography. Clinical Spine Surgery, 4(2), 183-187.

Watkins, J. (2010). Structure and function of the musculoskeletal system. Human Kinetics 1.

White III, A.A., Panjabi, M.M.(1990). Clinical Biomechanics of the Spine, second ed. Lippincott Williams & Wilkins.

Chapter 3: Nucleus Size and Position Measurements

3. 1. Introduction

Most of the numerical studies of the lumbar spine used the proportion of 44% for the nucleus and 56% for the annulus with the nucleus center being in the center of the disc (Naserkhaki et al. 2017a, 2017b; El-Rich et al., 2009; Shirazi-Adl, 1994; Breau et al., 1991). Variation of the intervertebral disc geometry can however affect the spinal load-bearing of the spine. This study used MR images of several individuals to investigate inter-individual variation of size and position of the nucleus at level L4-L5 of the spine. The obtained results were utilized in the following chapters to develop FE models of the FSU L4-L5 with various sizes and positions of the nucleus in order to investigate the effect of inter-individual variation of these parameters on the mechanical response of segment.

3.2. Methods

With ethics approval, the existing MRI data of 24 subjects aged between 21 to 84 years old taken for other reason than back pain were collected from the University of Alberta Hospital database. MRI scans were performed on a 64-slice scanner (Siemens/ Avanto) with slice thickness of 1.2 mm. Each patient was oriented in the head-first supine position. The subjects were 11 females and 13 males with mean ages of 57.9 and 47.75 years respectively. The MRI scans, as DCOM images, were imported into the medical image processing software Mimics (MIMICS Research17.0, Materialise, Belgium), to reconstruct 3D models of the subjects' L4-L5 intervertebral discs. The nucleus pulposus which is the central part of each intervertebral disc was distinguished by a high-intensity signal while the annulus fibrosis was identified using a low-intensity signal (Fig. 3.1).

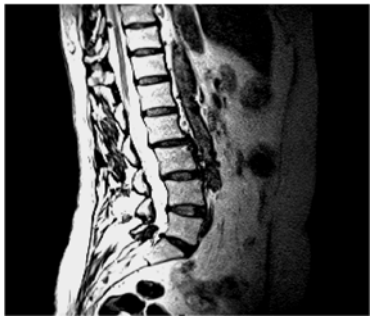

Fig. 3.1. Image of adolescent spine in the sagittal plane

A new mask was created for the outline of the nucleus zone with selecting L4-L5 intervertebral high-intensity portion. The whole L4-L5 intervertebral disc boundary between L4 and L5 vertebral bodies was detected as well. The masks for the nucleus and the whole disc were edited in each slice in the sagittal and coronal planes, and their 3D models were obtained using the "Calculate 3D" option in Mimics (Fig. 3.2a). Using the software Geomagic (Geomagic Control, 2014, 3D Systems, USA), the 3D models were smoothed and cleaned using the "Remove Spikes" and "Relax" tools to get high-quality models without affecting the geometry details (Fig. 3.2b).

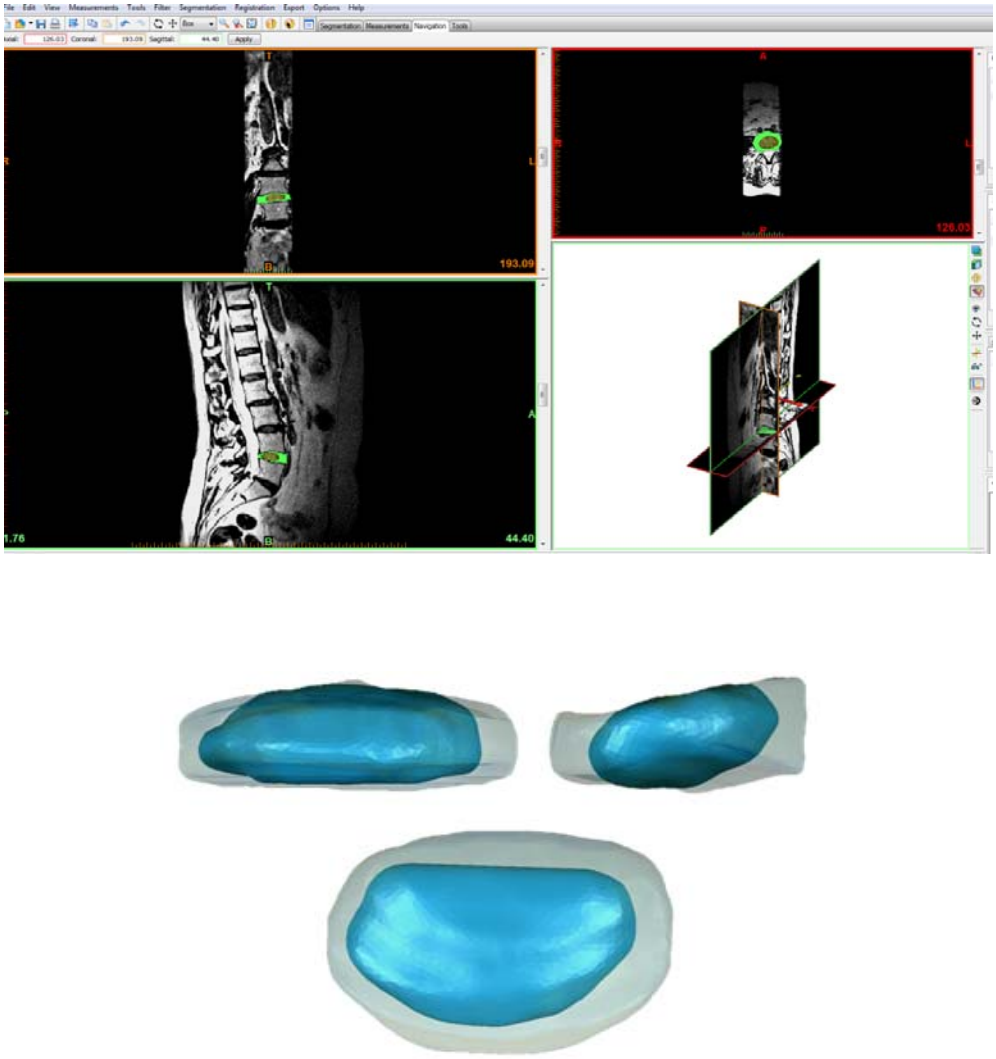

Fig. 3.2**.** 3D geometry acquisition of the L4-L5 intervertebral disc. (a) segmentation, (b) 3D geometry of the nucleus and whole disc

For All subjects, the cross-sectional area of the nucleus pulposus and the whole disc were measured using Geomagic's "Best Fit Plane" option. This option ignores the outliers and then passes the best fit through the rest of the points using an average of that points. Using Geomagic control, the positions of the nucleus and intervertebral disc centroid were computed as well.

3.3. Results

Table 3.1 summarizes the mean, median, standard deviation, min and max of size and position of nucleus center with respect to the disc center of the 24 individuals. The nucleus size was defined as a percentage of the total cross-section area of the disc, and the nucleus position was expressed as the distance between the center of the disc and center of the nucleus in the anterior-posterior direction. The positive sign of the nucleus position means that the nucleus center was posterior to the disc center while negative sign refers to the anterior position of the nucleus center.

Table 3.1**.** The Statistics for the nucleus size and positions of nucleus of 24 subjects.

	Mean	**Median**	**Std. Dev.**	**Min**	**Max**
Nucleus Size (%)	45.29	44.45	7.79	31.43	56.86
Nucleus Position (mm)	1.09	1.37	1.39	-1.67	3.26

The variations of the nucleus size and position among the 24 individuals are presented in Fig. 3.3a and b respectively. The results showed that the proportion of the nucleus cross-sectional area to the whole disc for all subjects was about 31% to 57%, and the location of the nucleus centroid varied between 1.67 mm anteriorly to 3.26 mm posteriorly with respect to the centroid of the whole disc.

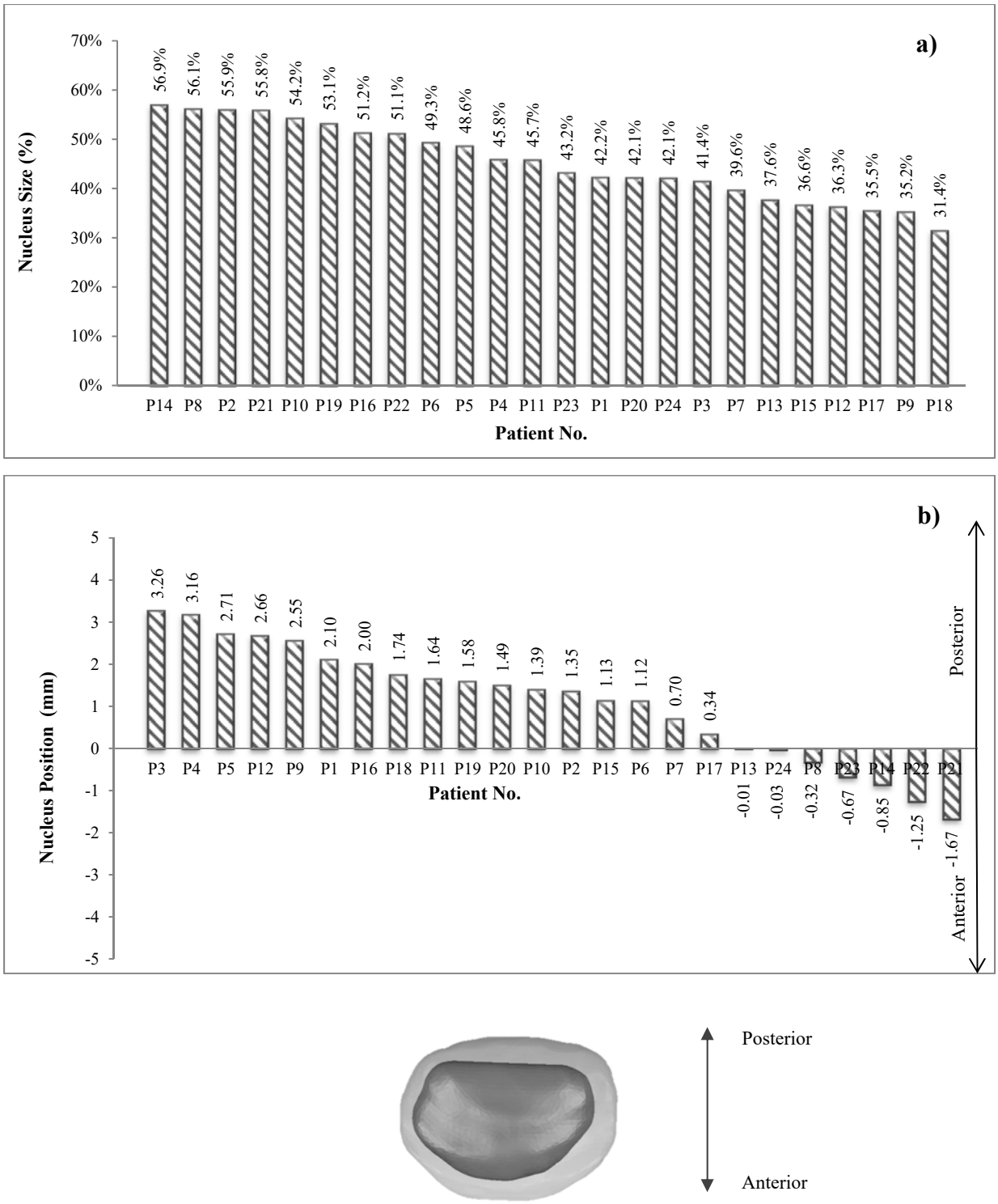

Fig. 3.3. L4-L5 nucleus size and position variations for 24 individuals. (a) proportion of the nucleus cross-sectional area to the whole disc area (%). (b) the difference between nucleus centroid and disc centroid in anterior-posterior direction(mm).

Fig. 3.4 shows how the nucleus size; nucleus position and age are correlated to each other. The correlation rank for each comparison is based on the R^2 values. R^2 is a statistical measure that varies between 0 and 1.0, where closer to 1.0 indicates a stronger correlation, while closer to 0 shows a weaker correlation. It was observed the nucleus size and the nucleus position (Fig. 3.4a) correlated poorly together (R^2 value of 0.1152). Furthermore, no correlation between the nucleus size and age (R^2 value of 0.0117) and between the nucleus position and age (R^2 value of 0.0233) was observed (Fig. 3.4b and c).

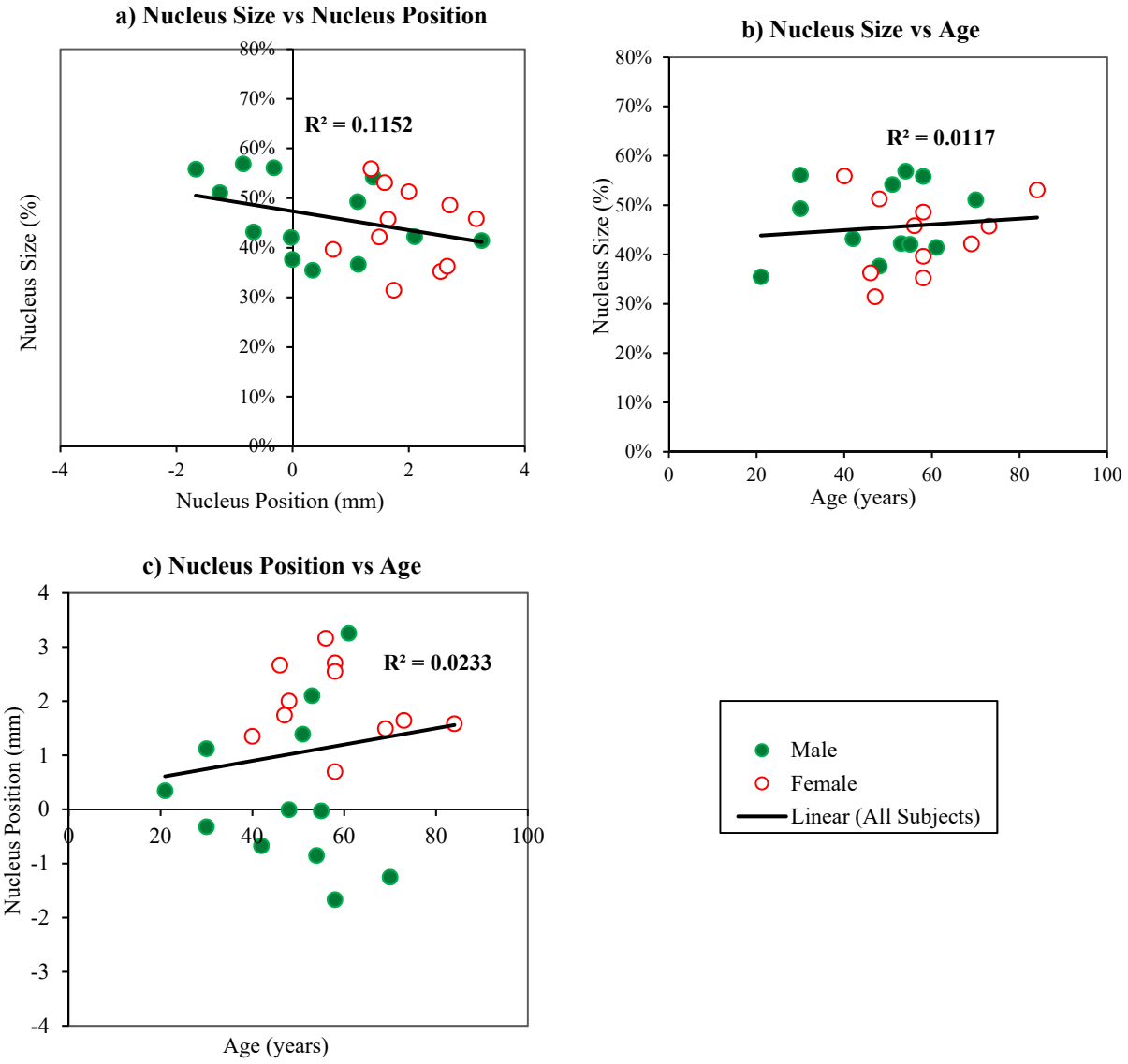

Fig. 3.4. The nucleus size, nucleus position, and age relationship. (a) the nucleus size and position correlation. (b) the nucleus size and age correlation. (c) the nucleus position and age correlation.

3.4. Discussion

In the current study, it should be noted that the nucleus size was defined as a proportion of the nucleus cross-sectional area to total cross-section area of the disc, similar to the literature (Schmidt et al., 2006; White III & Panjabi, 1990; Shirazi-Adl et al., 1984). Table 3.1 summarizes the range of the nucleus size and position variation reported in the literature. The results of the proportion of nucleus to disc cross-sectional area fell into the range reported in previous studies (Shirazi-adl et al., 1984). Their range however, was wider than the one reported in the literature (White III & Panjabi, 1990; Markolf & Morris, 1974; Nachemson, 1960). The results of the present study showed similar tendencies to those reported by Schmidt et al. (2006). The mean value of the nucleus sizes of four intervertebral disc specimens reported by Pooni et al. (1986) was almost the same as the mean value of the 24 subjects obtained in this study.

Schmidt at al. (2006) found that the center of the nucleus was located 3.5 mm posteriorly while O'Connell et al. (2007) reported that the nucleus center was located 1.17 mm towards the posterior side of the disc centre. Both of these two findings about the location of the nucleus are within or near the range of the nucleus position obtained in the current study.

Table 3.2**.** The range of nucleus size and position variation in human intervertebral disc

References	Nucleus Size	Nucleus Position
O'Connell et al., 2007	28%	1.17 mm posterior side of the disc center
Schmidt et al., 2006	44%	3.5 mm posterior side of the disc center
White III & Panjabi, 1990	30%-50%	Between the centre of the disc and posterior thirds of the sagittal diameter
Pooni et al., 1986	44%	-
Shirazi-adl et al., 1984	30%-60%	-
Markolf & Morris, 1974	50%-60%	In the posterior side of the disc center
Nachemson, 1960	50%	-

Furthermore, the relationships between the nucleus size and position; nucleus position and age; and nucleus size and age were investigated in this study and poor correlation was obtained between the nucleus size and position while no correlation was found between the nucleus size and age and between the nucleus position and age.

This study quantified the variations of the nucleus size and position among individuals. It recommends hence to consider these geometrical variations in computational biomechanics of the human spine.

References

El-Rich, M., Arnoux, P. J., Wagnac, E., Brunet, C., & Aubin, C. E. (2009). Finite element investigation of the loading rate effect on the spinal load-sharing changes under impact conditions. Journal of biomechanics, 42(9), 1252-1262.

Jacobs, N. T., Cortes, D. H., Peloquin, J. M., Vresilovic, E. J., & Elliott, D. M. (2014). Validation and application of an intervertebral disc finite element model utilizing independently constructed tissue-level constitutive formulations that are nonlinear, anisotropic, and time-dependent. Journal of biomechanics, 47(11), 2540-2546.

Markolf, K. L., & Morris, J. M. (1974). The Structural Components of the Intervertebral Disc: A study of their contributions to the ability of the disc to withstand compressive forces. JBJS, 56(4), 675-687.

Nachemson, A. (1960). Lumbar intradiscal pressure: experimental studies on post-mortem material. Acta Orthopaedica Scandinavica, 31(sup43), 1-104.

Naserkhaki, S., & El-Rich, M. (2017a). Sensitivity of lumbar spine response to follower load and flexion moment: finite element study. Computer methods in biomechanics and biomedical engineering, 20(5), 550-557.

Naserkhaki, S., Arjmand, N., Shirazi-Adl, A., Farahmand, F., & El-Rich, M. (2017b). Effects of eight different ligament property datasets on biomechanics of a lumbar L4-L5 finite element model. Journal of Biomechanics.

Naserkhaki, S., Jaremko, J. L., & El-Rich, M. (2016a). Effects of inter-individual lumbar spine geometry variation on load-sharing: Geometrically personalized finite element study. Journal of Biomechanics, 49(13), 2909-2917.

Naserkhaki, S., Jaremko, J. L., Adeeb, S., & El-Rich, M. (2016b). On the load-sharing along the ligamentous lumbosacral spine in flexed and extended postures: Finite element study. Journal of biomechanics, 49(6), 974-982.

Noailly, J., Wilke, H. J., Planell, J. A., & Lacroix, D. (2007). How does the geometry affect the internal biomechanics of a lumbar spine bi-segment finite element model? Consequences on the validation process. Journal of biomechanics, 40(11), 2414-2425.

O'Connell, G. D., Vresilovic, E. J., & Elliott, D. M. (2007). Comparison of animals used in disc research to human lumbar disc geometry. Spine, 32(3), 328-333.

Pooni, J. S., Hukins, D. W., Harris, P. F., Hilton, R. C., & Davies, K. E. (1986). Comparison of the structure of human intervertebral discs in the cervical, thoracic and lumbar regions of the spine. Surgical and Radiologic Anatomy: SRA, 8(3), 175-182. doi:10.1007/BF02427846

Schmidt, H., Heuer, F., Simon, U., Kettler, A., Rohlmann, A., Claes, L., & Wilke, H. J. (2006). Application of a new calibration method for a three-dimensional finite element model of a human lumbar annulus fibrosus. Clinical Biomechanics, 21(4), 337-344.

Shirazi-adl, S. A., Shrivastava, S. C., & Ahmed, A. M. (1984). Stress Analysis of the Lumbar Disc-Body Unit in Compression A Three-Dimensional Nonlinear Finite Element Study. Spine, 9(2), 120-134.

White III, A.A., Panjabi, M.M. (1990). Clinical Biomechanics of the Spine, second ed. Lippincott Williams & Wilkins.

Chapter 4: Finite Element (FE) Modeling

Introduction

Five FE models of the FSU L4-L5 with similar vertebrae and ligament but five different sizes and positions of the nucleus with respect to the disc were created. These sizes and positions were taken from the *in-vivo* values detailed in Chapter 3. This chapter explains the step-by-step method used to create these models, while the analyses and results will be discussed in the next chapter.

4.1. Geometry acquisition

The three-dimensional geometry of the vertebrae L4 and L5 was reconstructed from the CT-Scan images of a 20-year-old healthy male with a slice thickness of 1 mm taken from the University of Alberta Hospital database (Naserkhaki & El-Rich, 2017a; Naserkhaki et al. 2016a, 2016b, 2017b).

4.2. Mesh

The reconstructed geometry was imported into the software Hypermesh (Hyperworks 14.0, Altair, USA) to mesh the vertebrae and to create the ligament and the intervertebral disc including the nucleus, annulus and collagen fibers. Each vertebra included two endplates, posterior elements, and facet joints (Fig. 4.1)

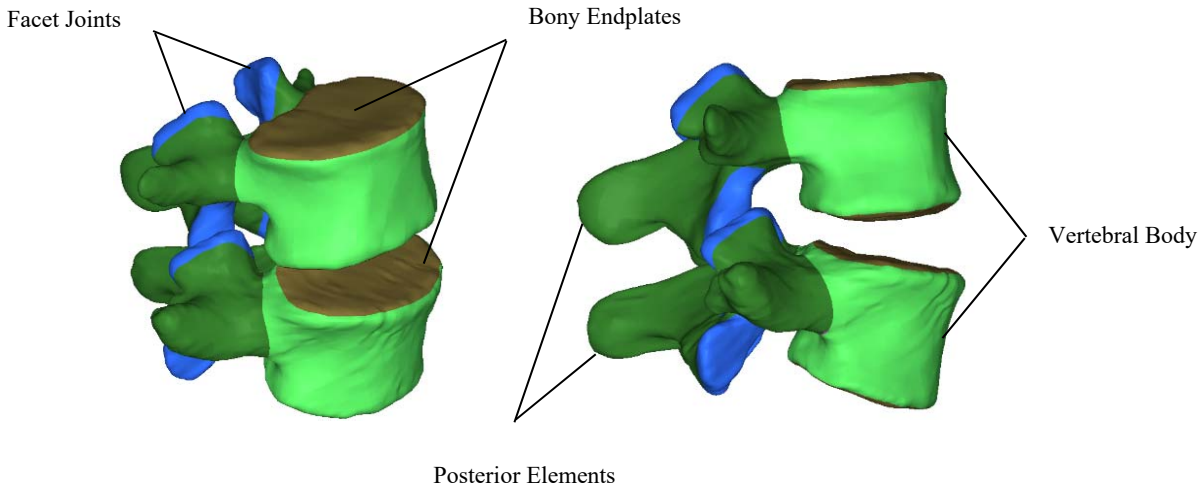

Fig. 4.1. Lumbar vertebrae L4 and L5

Four discs with distinct nucleus sizes and positions were selected for the FE modeling according to the obtained ranges of the sizes and positions of the nucleus as summarized in Table 4.1. In addition, one case with nucleus size proportion of 44% and center located in the center of the disc (Model 44) was modeled. This disc geometry has been reported by Pooni et al. (1986) and Breau et al. (1991) and used by previous FE studies (Naserkhaki et al. 2017a, b; El-Rich et al., 2009; Shirazi-Adl, 1994). The proportion of the cross-sectional area of nucleus and annulus as well as the position of the nucleus center were changed according to the cases studied while the height and cross-sectional area of the whole disc were kept constant during all analyses.

Table 4.1. Size and position of the nucleus with respect to the whole disc for each model

Model	Nucleus Size	Nucleus Position
Model 31	31 %	Center
Model 44	44 %	Center
Model 57	57 %	Center
Model 44-1.5A	44%	1.5 mm - Anterior
Model 44-3.25 P	44%	3.25 mm- Posterior

In order to generate the intervertebral disc, the inferior endplate of the vertebra L4 and the superior endplate of the vertebra L5 were divided into two regions to separate the nucleus from the annulus. To be able to change the nucleus size, the outline of the nucleus was created in the central part of the disc and its perimeter was chosen according to the selected sizes. The position of the nucleus was changed by moving its center in the anterior-posterior directions according to the positions selected.

After separating the areas of the nucleus and annulus in the endplates, they were meshed with 4 – node shell elements and used to extrude seven layers of 8-node (brick) element to create the nucleus and annulus (Fig. 4.2, Fig. 4.3).

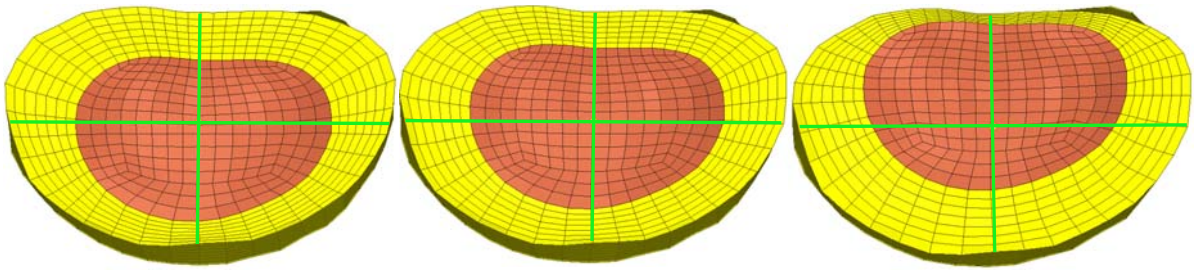

Fig. 4.2. Various positions of the nucleus with respect to the disc

The elements of the annulus were reinforced by eight crisscross layers of annular fibers modeled using unidirectional springs that resist tension only (Fig. 4.3). The orientation of the fibers was arranged to incline alternatively at an angle close to ±35° to the horizontal plane (Naserkhaki et al. 2016a, 2016b, 2017b; El-Rich et al., 2009; Schmidt et al., 2007b; Shirazi-Adl et al., 1984; Natarajan & Andersson, 1999).

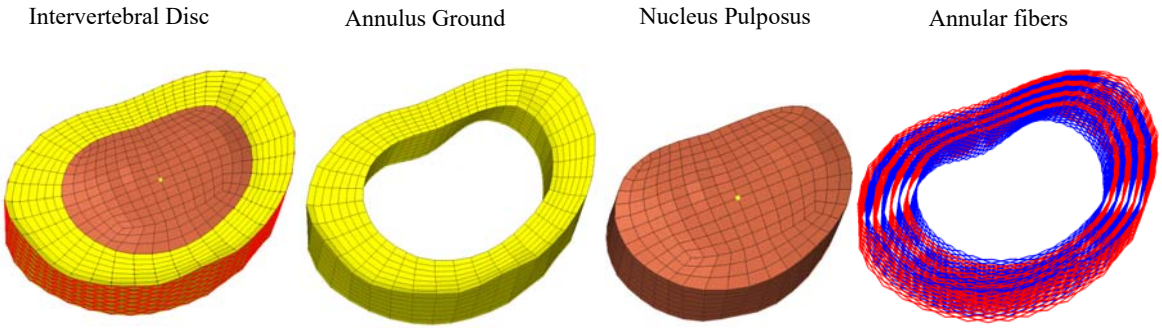

Fig. 4.3.The components of the intervertebral disc

After generating the intervertebral disc between two endplates, the meshes of the adjacent endplates were converted into 3-node shell elements by dividing each 4-node shell element into two 3-node shell elements. The superior endplate of the vertebra L4, the inferior endplate of the vertebra L5 were also meshed with 3-node shell elements. The cortical bone, which is also known as a compact bone covering the outer surface of vertebrae, was meshed with 3-node shell elements. The cortical bone was then filled by cancellous bone, also called "trabecular bone" or "spongy bone" using 4-node tetrahedral solid elements (Naserkhaki et al. 2016a, 2016b, 2017b, El-Rich et al., 2009). The mesh of all spinal components was continuous, i.e. neither kinematic coupling nor tie option between the nodes were used.

The surrounding ligaments including the Anterior Longitudinal Ligament (ALL), Posterior Longitudinal Ligament (PLL), Capsular Ligament (CL), Transvers Ligament (ITL), Supraspinous Ligament (SSL), Interspinous Ligament (ISL), and Ligamentum Flavium (LF) were simulated by one-dimensional, nonlinear unidirectional springs resisting tension only (Naserkhaki & El-Rich, 2017a; Naserkhaki et al. 2016a, 2016b; Breau et al., 1991). These ligaments are shown in Fig. 4.4. The details of ligament modeling are described as follows (Naserkhaki et al., 2016b; El-Rich et al., 2009):

ALL: Five parallel springs connecting the anterior side of adjacent endplates (the inferior endplate of the vertebra L4 and the superior endplate of the vertebra L4) with attachments to the disc.

PLL: Three parallel springs connecting the posterior edge of adjacent endplates with attachments to the disc.

CL: Eight springs attaching the periphery of every adjacent facet surface (superior tip of the facet articulation of the vertebra L5 to the inferior tip of the facet articulation of the vertebra L4).

LF: Three parallel springs connecting the laminae of adjacent vertebrae (The inferior laminae of the vertebra L4 and the superior laminae of the vertebra L5).

ISL: Four parallel springs attaching adjoining spinous processes (The inferior spinous process of the vertebra L4 and the superior spinous process of the vertebra L5)

SSL: Three parallel springs connecting the posterior tips of adjacent spinous processes

ITL: Two parallel springs attaching adjacent transverse processes

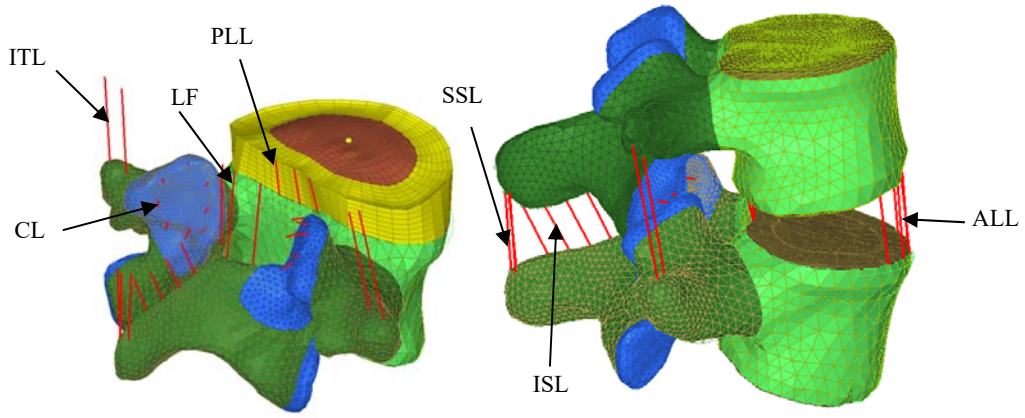

Fig. 4.4. Ligaments details in the FE model

4.3. Material properties

The material properties of various components were taken from the literature (Table 4.2, 4.3, 4.4, 4.5).

Bony components (L4 & L5 vertebrae)

Although bone is a nonlinear viscoelastic material, a simple linearly isotropic elastic material was used in the FE models to simulate the cortical bone, cancellous bone and cartilaginous endplates as this study investigates the response of FSU to static loading conditions (Naserkhaki et al., 2016b; Goto et al., 2003). The material properties used in the vertebrae modeling are presented in Table 4.2.

Table 4.2.Material properties of the bony structures (L4 & L5 vertebrae)

Material	Material Behavior	Mechanical Properties		References
Cortical bone	Linear elastic	E = 12,000 MPa	v = 0.30	Naserkhaki et al., 2016 a, 2016b, 2017b; Schmidt et al., 2007b; Goto et al., 2003
Cancellous bone		E = 200 MPa	v = 0.315	
Cartilaginous Endplate		E= 23.8 MPa	v = 0.4	

Intervertebral disc

The annulus fibrosus was simulated as a matrix of a homogeneous ground substance reinforced by annular fibers and the nucleus pulposus as a gelatinous incompressible core. Both components were governed by isotropic, incompressible, hyper-elastic first-order Mooney-Rivlin (C_{01}, C_{10}) formulation (Naserkhaki et al., 2016b, 2017b; El-Rich et al., 2009; Schmidt et al., 2007) with the following strain energy function W :

$W = C_{10}(I_1 - 3) + C_{01}(I_2 - 3)$

C_{01}, C_{10} material constants

I_1, I_2 first and second invariants of the deviatoric strain tensor

The material properties used in the disc modeling are summarized in Table 4.3.

Table 4.3**.** Material properties of the intervertebral disc's components

Material	Material Behavior	Mechanical Properties		References
Nucleus pulposus	Hyper-elastic(Mooney-Rivlin)	C10 = 0.12	C01=0.030	Naserkhaki et al., 2016 a, 2016b, 2017; El-Rich et al., 2009; Schmidt et al., 2007b
Annulus ground substance		C10 = 0.18	C01=0.045	
Annular fibers	Nonlinear force-displacement curve			Shirazi-Adl et al., 1984, 1986; Schmidt et al, 2006; Naserkhaki et al., 2016a, 2016b,2017b

The overall volume of the annular fibers was assumed to occupy 16% of the total annulus volume. Both modulus of elasticity and cross-sectional area of the fibers were assumed to increase radially through thickness of annulus with the maximum value being in the outer layers of the annulus (Naserkhaki et al. 2016a, 2016b, 2017b; El-Rich et al., 2009; Schmidt et al., 2007b; Shirazi-Adl et al, 1984; Natarajan & Andersson, 1999). The ratio of cross-sectional area and elasticity constants of the eight layers of the annular fibers are detailed in Table 4.4.

Table 4.4. Distribution of annular fibers properties in each layer (Shirazi-Adl et al., 1986)

Location of Fibers	Ratio of cross-sectional areas	Ratio of elasticity constants
Inner layers	0.47	0.65
Middle layers	0.62	0.75
	0.78	0.9
Outer layers	1	1

The nonlinear force-displacement curves developed from the stress-strain curve (Fig. 4.5), reported by Schmidt et al. (2006), and Shirazi-Adl et al. (1986) were used to model the annular fibers (Naserkhaki et al., 2016b, 2017b).

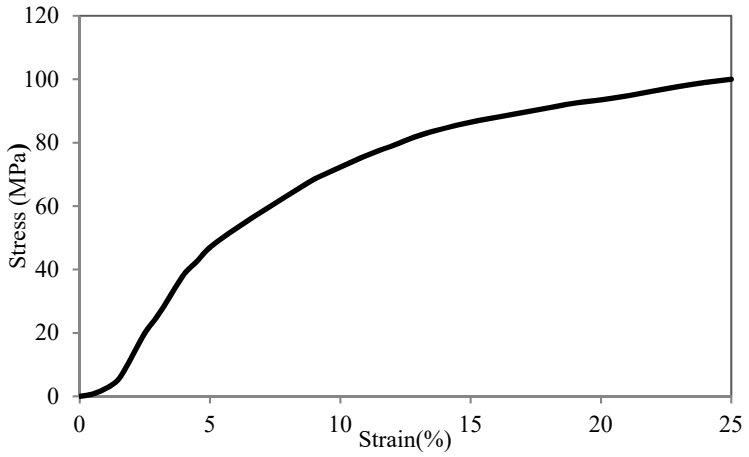

Fig. 4.5. Stress–strain curve for the annular collagenous fibers (Shirazi-Adl et al., 1986) (Figure is reproduced).

For each FE model, the overall volume of the annulus was calculated. As the annular fibers make about 16% of the total annulus volume and according to the ratio of cross-sectional area for each layer of the annular fibers (Shirazi-Adl et al., 1986), the length and cross-sectional area of each layer were calculated. Using the stress-strain curve (Shirazi-Adl et al., 1986; Schmidt et al., 2007b) and the calculated cross-sectional area of the annular fibers in each layer, the forces were obtained by multiplying the stress by the cross-sectional area and the ratio of elasticity for each layer. The displacements were determined as well by multiplying the strain by the length of annular fibers. The force-displacement curves for all five models are illustrated in Fig. 4.6.

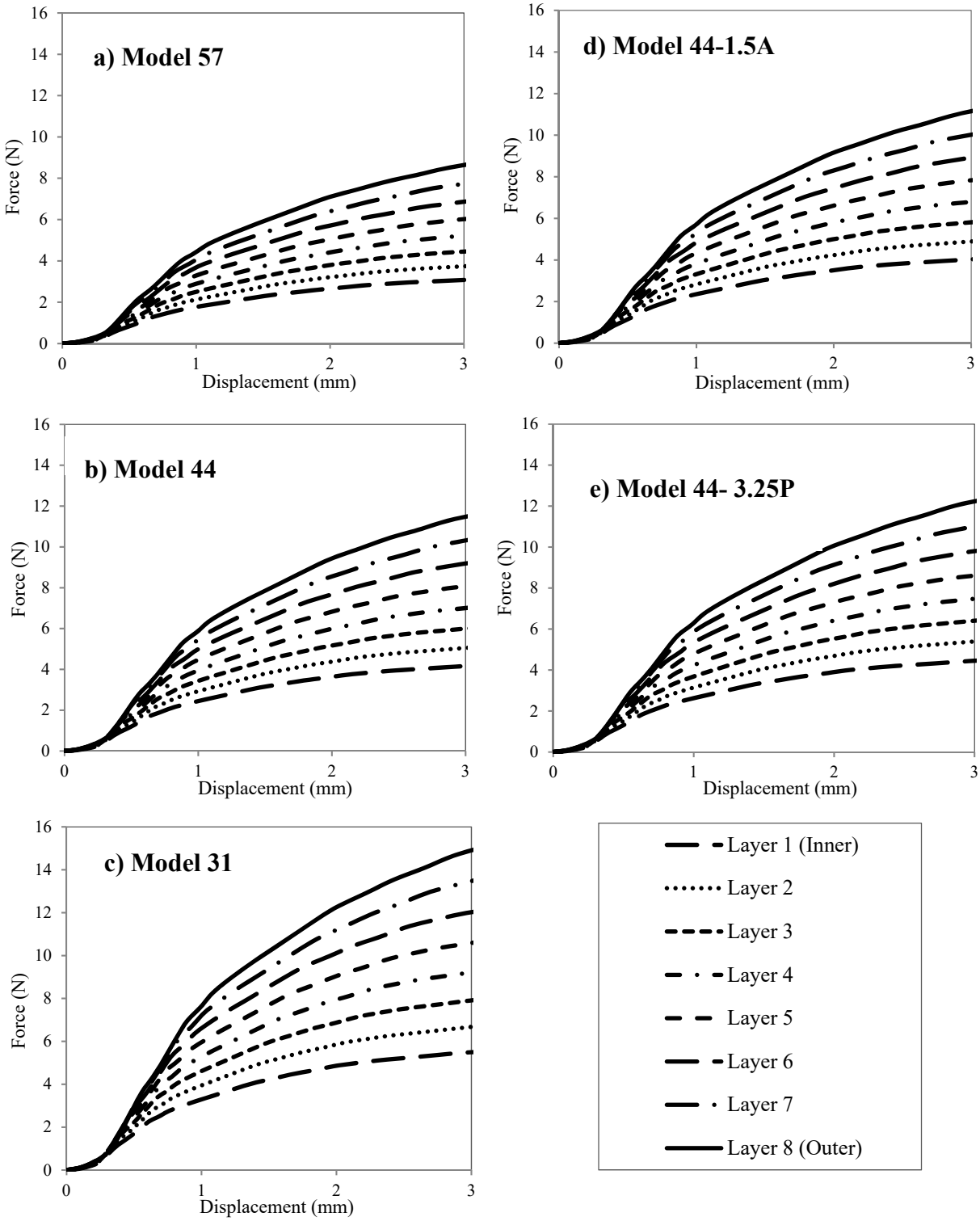

Fig. 4.6. Force-displacement curve of the annular fibers for: (a) Model 57, (b) Model 44, (c) Model 31, (d) Model 44-1.5A, (e) Model 44-3.25P

Ligaments

The nonlinear properties (Rohlmann et al., 2006) used to simulate the ligaments are summarized in Table 4.5

Table 4.5 Nonlinear stiffness of the spinal ligaments (Rohlmann et al., 2006).

Ligaments	Stiffness (N/mm)	Strains (%)	Stiffness (N/mm)	Strains (%)	Stiffness (N/mm)	Strains higher than (%)
ALL	347	0-12.2	787	12.2-20.3	1864	20.3
PLL	29.5	0-11.1	61.7	11.1-23	236	23
CL	36	0-25	159	25-30	384	30
LF	7.7	0-5.9	9.6	5.9-49	58.2	49
ISL	1.4	0-13.9	1.5	13.9-20	14.7	20
SSL	2.5	0-20	5.3	20-25	34	25
ITL	0.3	0-18.2	1.8	18.2-23.3	10.7	23.3

Facet joints

The joints between the inferior articular processes of the vertebra L4 and the superior articular processes of the vertebra L5 are called the facet joints or articular joints. They were modeled by a frictionless surface-to-surface contact (Naserkhaki et al. 2016b, 2017b; El-Rich et al., 2009; Schmidt et al., 2007b).

4.4. Loading and boundary conditions

The superior endplate and facet joints of L4 and the inferior end plate and facet joints of the L5 were constrained as two rigid bodies. The moments were applied to the reference point located in the center of the superior endplate of the vertebra L4 (Fig. 4.7). The inferior endplate and facet joints of the vertebra L5 were fixed (Naserkhaki et al. 2017; Heuer et al., 2007a, 2007b; Schmidt et al., 2007b). To compensate the muscle forces ignored in the simulations, a compressive follower load (FL) whose line of action passes through the center of L4 and L5 vertebral bodies was applied (Naserkhaki et al., 2016b; Schmidt et al., 2007b; Shirazi-Adl, 2006; Patwardhan et al., 1999).

In order to better understand the effect of nucleus size and position on the response of the FSU, different load combinations were used in this study (Table 4.6). In cases 3 and 4, the resulting moment of two moments applied in the anatomical planes like flexion and lateral bending moments for instance, was always 10Nm about an oblique spatial axis (Schmidt et al., 2007b). In total, 32 loading scenarios were defined and applied to compare the intervertebral rotation (IVR), IDP, and maximum annular fibers strain.

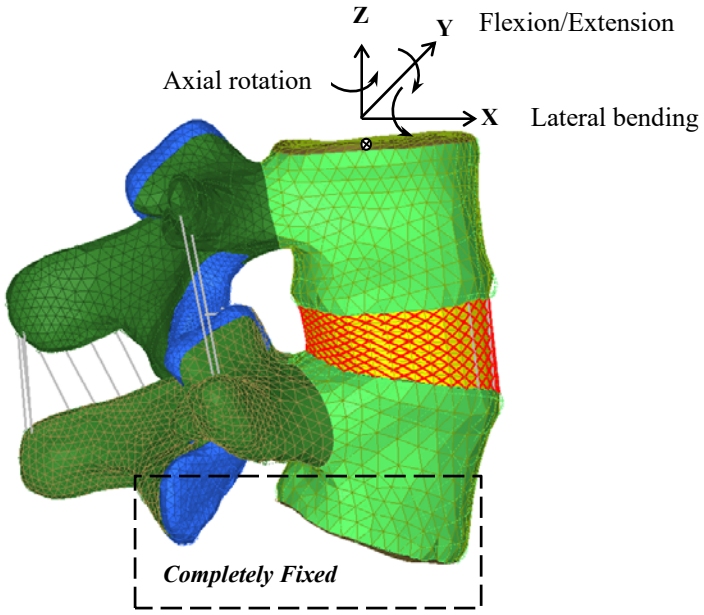

Fig. 4.7**.** Details of loading and boundary conditions

Table 4.6 Loading scenarios

Load Cases	Load Combinations	FL (N)	Moment (Nm)	Description	References
Case 1	Pure moment	-	10	Flexion(FLX), extension (EXT), right lateral bending (RLB), left lateral bending (LLB), right axial rotation (RAR), left axial rotation (LAR)	Panjabi et al., 1994
Case 2	FL+ Moment	500	10	FL+FLX, FL+EXT, FL+RLB, FL+LLB, FL+LAR, FL+RAR	Heuer et al., 2007a, 2007b
Case 3	FL+FLX/EXT+RLB	500	10	The direction of the resulting moment (10 Nm) changed gradually every 15^{o} from FLX or EXT to RLB	Schmidt et al., 2007b
Case 4	FL+FLX/EXT+LAR	500	10	The direction of the resulting moment (10 Nm) changed gradually every 15^{o} from FLX or EXT to LAR	Schmidt et al., 2007b

4.5. Validation

The model with 44% proportion of the nucleus and center located in the center of the disc has recently been validated by Naserkhaki et al. (2017b), and it was in good agreement with other *in-vitro* studies. The validation of Model 44 is briefly explained here:

- The aforementioned study investigated the effects of eight distinct ligament properties on the response of a single FE model of the FSU L4-L5. This model which is similar to Model 44 was validated against *in-vitro* and *in-vivo* data.

- The boundary conditions defined for the FSU L4-L5 are similar to the ones used in the current study.

- All the material properties used in the validation process are the same as those in the current study except ligament properties. For the ligament, eight different sets of ligament properties derived from the previous studies were used to create eight distinct models. The dataset reported by Rohlmann et al. (2006) was used in Model 44 as the predictions provided the best alignment with *in-vitro* rotation (Heuer et al., 2007a, 2007b), IDP (Andersson and Schultz, 1979), and ligament strains (Panjabi et al., 1982).

- The predicted responses (IDP, RoM, and ligament forces and strains) of the FE model with Rohlmann et al. (2006) ligament property datasets (similar to the Model 44 in the current study) were compared to *in-vitro* data in Fig. 4.8 and Fig. 4.9 (Naserkhaki et al., 2017b).

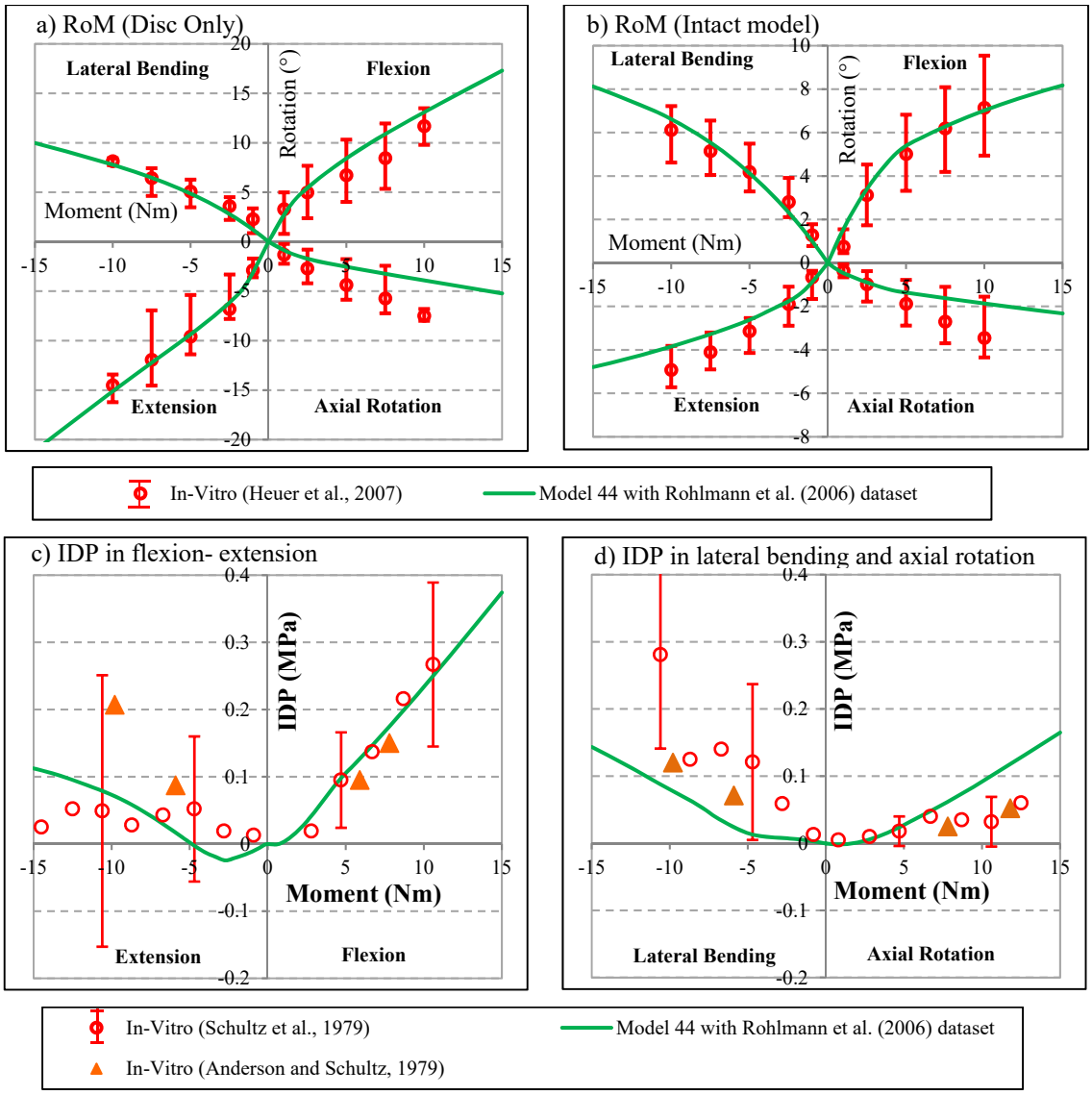

Fig. 4.8. L4-L5 FSU validation. (a) RoM of the disc-alone model, (b) RoM of intact model with disc, ligaments and facet joints under pure moment, (c-d) relative changes in IDP of the intact model under moment in presence of 400 N FL (Naserkhaki et al., 2017b).

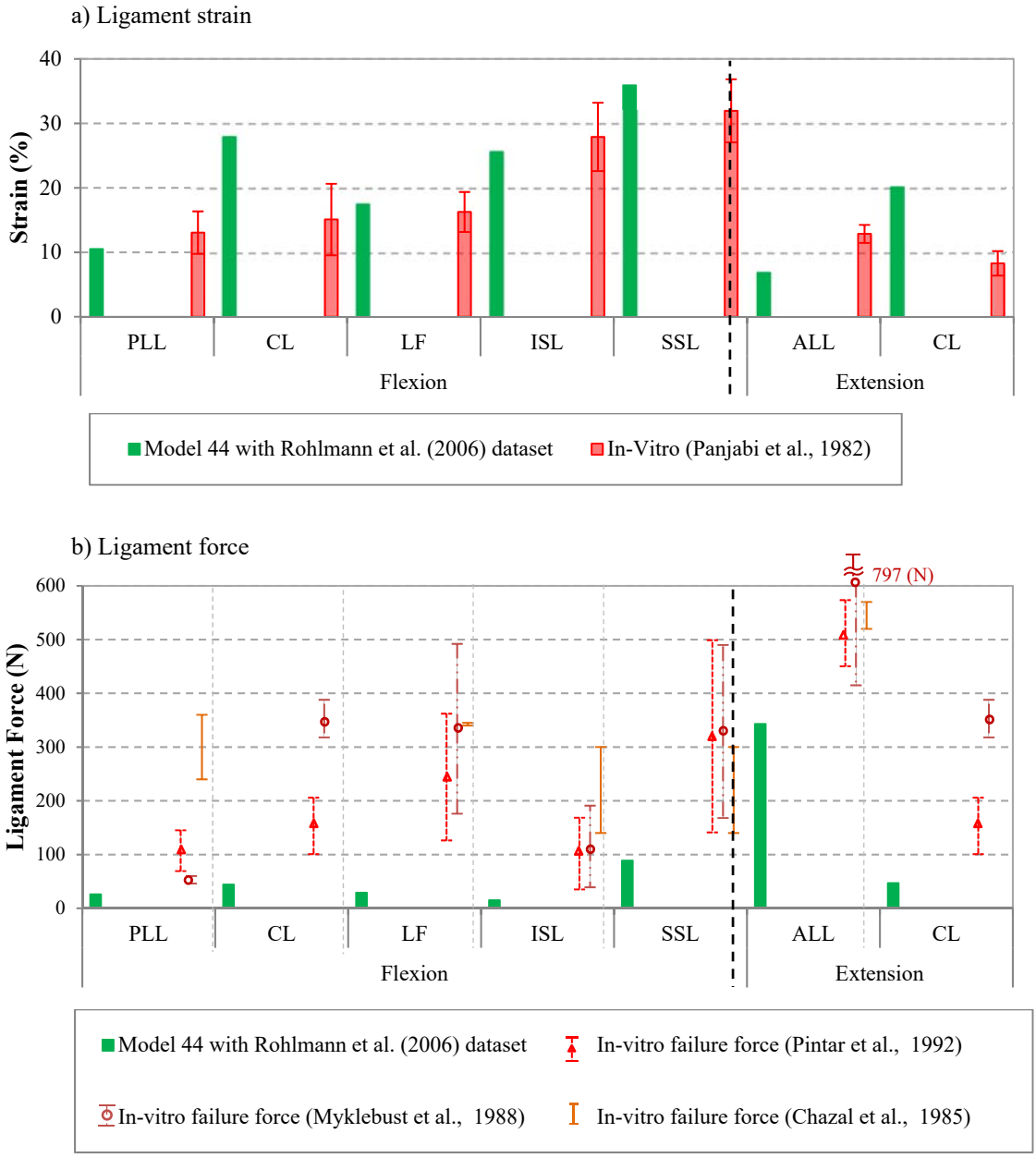

Fig. 4.9. L4-L5 FSU validation. (a) ligament strain, (b) ligament force under flexion and extension moments of 15 Nm. Ligament forces are resultant force of all springs for each ligament after the vector summation rule (Naserkhaki et al., 2017b)

References

Andersson, G. B., & Schultz, A. B. (1979). Effects of fluid injection on mechanical properties of intervertebral discs. Journal of biomechanics, 12(6), 453-458.

Breau, C., Shirazi-Adl, A., & De Guise, J. (1991). Reconstruction of a human ligamentous lumbar spine using CT images—a three-dimensional finite element mesh generation. Annals of biomedical engineering, 19(3), 291-302.

Chazal, J., Tanguy, A., Bourges, M., Gaurel, G., Escande, G., Guillot, M., & Vanneuville, G. (1985). Biomechanical properties of spinal ligaments and a histological study of the supraspinal ligament in traction. Journal of biomechanics, 18(3), 167-176.

El-Rich, M., Arnoux, P. J., Wagnac, E., Brunet, C., & Aubin, C. E. (2009). Finite element investigation of the loading rate effect on the spinal load-sharing changes under impact conditions. Journal of biomechanics, 42(9), 1252-1262.

Goto, K., Tajima, N., Chosa, E., Totoribe, K., Kubo, S., Kuroki, H., & Arai, T. (2003). Effects of lumbar spinal fusion on the other lumbar intervertebral levels (three-dimensional finite element analysis). Journal of Orthopaedic Science, 8(4), 577-584.

Heuer, F., Schmidt, H., Klezl, Z., Claes, L., & Wilke, H. J. (2007a). Stepwise reduction of functional spinal structures increase range of motion and change lordosis angle. Journal of biomechanics, 40(2), 271-280

Heuer, F., Schmidt, H., Claes, L., & Wilke, H. J. (2007b). Stepwise reduction of functional spinal structures increase vertebral translation and intradiscal pressure. Journal of biomechanics, 40(4), 795-803.

Myklebust, J. B., Pintar, F., Yoganandan, N., Cusick, J. F., Maiman, D., Myers, T. J., & Sances Jr, A. (1988). Tensile strength of spinal ligaments. Spine, 13(5), 528-531.

Naserkhaki, S., & El-Rich, M. (2017a). Sensitivity of lumbar spine response to follower load and flexion moment: finite element study. Computer methods in biomechanics and biomedical engineering, 20(5), 550-557.

Naserkhaki, S., Arjmand, N., Shirazi-Adl, A., Farahmand, F., & El-Rich, M. (2017b). Effects of eight different ligament property datasets on biomechanics of a lumbar L4-L5 finite element model. Journal of Biomechanics.

Naserkhaki, S., Jaremko, J. L., & El-Rich, M. (2016a). Effects of inter-individual lumbar spine geometry variation on load-sharing: Geometrically personalized finite element study. Journal of Biomechanics, 49(13), 2909-2917.

Naserkhaki, S., Jaremko, J. L., Adeeb, S., & El-Rich, M. (2016b). On the load-sharing along the ligamentous lumbosacral spine in flexed and extended postures: Finite element study. Journal of biomechanics, 49(6), 974-982

Natarajan, R. N., Williams, J. R., & Andersson, G. B. (2004). Recent advances in analytical modeling of lumbar disc degeneration. Spine, 29(23), 2733-2741.

Panjabi, M.M., Oxland, TR., Yamamoto I., & Crisco, JJ. (1994). Mechanical behavior of the human lumbar and lumbosacral spine as shown by three-dimensional load-displacement curves. The Journal of Bone & Joint Surgery, 76(3), 413-424. doi:10.2106/00004623-199403000-00012

Panjabi, M. M., Goel, V. K., & Takata, K. (1982). Physiologic Strains in the Lumbar Spinal Ligaments: An In VitroBiomechanical Study. Spine, 7(3), 192-203.

Patwardhan, A. G., Havey, R. M., Meade, K. P., Lee, B., & Dunlap, B. (1999). A Follower Load Increases the Load-Carrying Capacity of the Lumbar Spine in Compression. Spine, 24(10), 1003-1009.

Pintar, F. A., Yoganandan, N., Myers, T., Elhagediab, A., & Sances, A. (1992). Biomechanical properties of human lumbar spine ligaments. Journal of biomechanics, 25(11), 1351-1356.

Pooni, J. S., Hukins, D. W., Harris, P. F., Hilton, R. C., & Davies, K. E. (1986). Comparison of the structure of human intervertebral discs in the cervical, thoracic and lumbar regions of the spine. Surgical and Radiologic Anatomy : SRA, 8(3), 175-182. doi:10.1007/BF02427846

Rohlmann, A., Bauer, L., Zander, T., Bergmann, G., & Wilke, H. J. (2006). Determination of trunk muscle forces for flexion and extension by using a validated finite element model of the lumbar spine and measured in vivo data. Journal of Biomechanics, 39(6), 981-989.

Schmidt, H., Kettler, A., Rohlmann, A., Claes, L., & Wilke, H. J. (2007a). The risk of disc prolapses with complex loading in different degrees of disc degeneration–a finite element analysis. Clinical Biomechanics, 22(9), 988-998.

Schmidt, H., Kettler, A., Heuer, F., Simon, U., Claes, L., & Wilke, H. J. (2007b). Intradiscal pressure, shear strain, and fiber strain in the intervertebral disc under combined loading. Spine, 32(7), 748-755

Schmidt, H., Heuer, F., Simon, U., Kettler, A., Rohlmann, A., Claes, L., & Wilke, H. J. (2006). Application of a new calibration method for a three-dimensional finite element model of a human lumbar annulus fibrosus. Clinical Biomechanics, 21(4), 337-344.

Shirazi-Adl, A. (2006). Analysis of large compression loads on lumbar spine in flexion and in torsion using a novel wrapping element. Journal of biomechanics, 39(2), 267-275.

Shirazi-Adl, A. (1994). Biomechanics of the lumbar spine in sagittal/lateral moments. Spine, 19(21), 2407-2414.

Shirazi-Adl, A. A. A. S. S., Ahmed, A. M., & Shrivastava, S. C. (1986). Mechanical response of a lumbar motion segment in axial torque alone and combined with compression. Spine, 11(9), 914-927.

Shirazi-adl, S. A., Shrivastava, S. C., & Ahmed, A. M. (1984). Stress Analysis of the Lumbar Disc-Body Unit in Compression A Three-Dimensional Nonlinear Finite Element Study. Spine, 9(2), 120-134.

Chapter 5: Effects of Nucleus Size and Position on the Response of the Lumbar Functional Spinal Unit L4-L5 to Complex Loading: Finite Element Analysis.

This chapter has been submitted as Fallahi Arezodar, F., Naserkhaki, S., Duke, K., Adeeb, S., El-Rich, M., 2017, to Journal of Biomechanics, the manuscript number BM-S-17-01730.

Abstract

Response of the lumbar spine to mechanical load, a major contributing factor in Low Back Pain (LBP), depends on the geometry of the spinal structures. This geometry varies among individuals and along the same spine. Understanding the effects of inter-individual variation of spinal geometry on the mechanical behavior of spine is very important and can be useful in LBP assessment. This study aimed to quantify variations of the position and size of the nucleus pulposus in the lumbar L4-L5 discs of 24 subjects using their MR images. The effects of these variations on response of the Functional Spinal Unit (FSU) L4-L5 to various load combinations were then investigated using Finite Element (FE) method. The proportion of the nucleus cross-sectional area to the whole disc for all subjects was found between 31% and 57% and the position of the nucleus centroid varied from 1.67 mm anteriorly to 3.26 mm posteriorly with respect to the centroid of the whole disc. Accordingly, five 3D nonlinear detailed FE models of the FSU L4-L5 with different sizes and positions of the nucleus were developed. The models were subjected to 10Nm moments with direction varying gradually by about 15^{o} between anatomical planes combined or not with 500N follower load (FL). The intradiscal pressure (IDP), annular fiber stains and intervertebral rotation (IVR) were predicted and compared. Overall, the nucleus size and position had slight effects on IVR and distinct influence on IDP and annular fibers strain depending on loading combination and direction.

Keywords: Low Back Pain, lumbar spine, intervertebral disc, nucleus, finite element analysis, follower load, intradiscal pressure, intervertebral rotation, annular fiber strains

5.1. Introduction

Many computational studies investigated the role of spinal components such as ligaments, articular facet joints and intervertebral discs in resisting loads (Naserkhaki et al., 2016a, 2016b; El-Rich et al., 2009; Jacobs et al., 2014; Noilley et al., 2007; Schmidt at al., 2007a, 2007b; Panjabi et al., 1994; Shirazi-Adl et al., 1986, 1984). These roles might be influenced by the geometry of the spinal structures (Naserkhaki et al., 2016a, 2016b) such as height and cross-sectional area of the intervertebral disc (Natarajan & Andersson, 1999) as well as size and position of the nucleus with respect to the disc (Naserkhaki et al., 2016a, 2016b; Schmidt et al., 2007b; Noilley et al., 2007). Some *in-vitro* studies investigated the variation of lumbar disc height and cross-sectional area among people and along the same spine (Pooni et al., 1986; O'Connell et al., 2007). Additionally, some *in-vitro* and numerical studies investigated the effects of these variations on the mechanical response of the spine (Meijer et al., 2011, Noilley et al., 2007; Natarajan & Andersson, 1999; Nachemson et al., 1979). In addition to height and cross-sectional area of the disc, Pooni et al. (1986) compared the shape of the disc and the orientation of the annular fibers along the spinal column and found that these geometrical parameters can affect possible mechanisms of failure of spinal structures. Natarajan and Andersson (1999) reported that discs with a small area to height ratio demonstrated larger motion, higher annular fiber stresses and much higher risk of failure as compared to discs with large ratio. Also, Nachemson et al. (1979) reported that the transverse cross-sectional area of the lumbar disc was smaller in women than men and, as a result, female segments experienced larger increase in IDP in response to compression load and were more flexible to bending and torsional moment than male segments.

The position and size of the nucleus with respect to the disc also vary among people, along the same spine, and with ageing (Pooni et al., 1986; Meijer et al., 2011, O'Connell et al., 2007). Shirazi et al. (1984) reported that cross-sectional area of the nucleus is about 30-60% of the whole disc. Schmidt at al. (2006) found that the nucleus occupies approximately 44% of the disc area and with the center located 3.5 mm posteriorly from the disc center. White III and Panjabi (1990) reported that the lumbar nucleus cross-sectional area is about 30-50% of the total disc cross-sectional area. Despite previous findings on the effects of variation of the disc geometry on the mechanical response of FSUs or the entire spine, there is still lack of knowledge on the effects of the inter-individual nucleus size and position variation on spinal response.

Therefore, this study aimed to: 1. Determine the size and position of the nucleus with respect to the disc at the lumbar level L4-L5 of 24 individuals using their MRI data and 2. Investigate the effects of the size and position of the nucleus on the mechanical response of the FSU L4-L5 to various load combinations using the FE method.

5.2. Materials and methods

Measurements of disc geometry

With ethics approval, MR images of the spines of 24 subjects (aged between 21 to 84 years) with slice thickness of 1.2 mm, already available at the University of Alberta Hospital database were collected and used to construct the 3D geometry of the L4-L5 disc using the software Mimics (MIMICS Research17.0, Materialise, Belgium)(Fig. 5.1a). After geometry cleaning and smoothing, the cross-sectional area of the nucleus and the whole disc as well as the position of the nucleus centroid with respect to the whole disc centroid in the anterior-posterior direction were measured using the software Geomagic Control (Geomagic Control, 2014, 3D Systems, USA). The size of the nucleus was expressed as a percentage of its cross-sectional area to the cross-sectional area of the whole disc.

Results showed that the size of the nucleus for all subjects ranged between 31% to 57% with mean value of 45.3%, median value of 44.5%, and standard deviation of 8% (Fig. 5.2a). The location of the nucleus centroid varied between 1.67 mm anteriorly to 3.26 mm posteriorly with respect to the centroid of the whole disc (Fig. 5.2b). No correlation between cross-sectional area and anterior-posterior position of the nucleus was obtained. Based on these results, four cases with various nucleus sizes and positions were studied using FE method as summarized in Table 5.1. In addition, one case with nucleus size proportion of 44% and centroid located in the center of the disc (Model 44) was modeled. This disc geometry has been reported by Pooni et al. (1986) and Breau et al. (1991) and used by previous FE studies (Naserkhaki et al. 2017a, 2017b; El-Rich et al., 2009; Shirazi-Adl, 1994).

Table 5.1 Selected cross-sectional area and position cases for FE modeling

	Position of the nucleus center with respect to the disc center			
% of NP x-sectional area/entire disc		1.5mm posteriorly	0	3.25mm anteriorly
	31%	-	Model 31	-
	44%	Model 44-1.5A	Model 44	Model 44-3.25P
	57%	-	Model 57	-

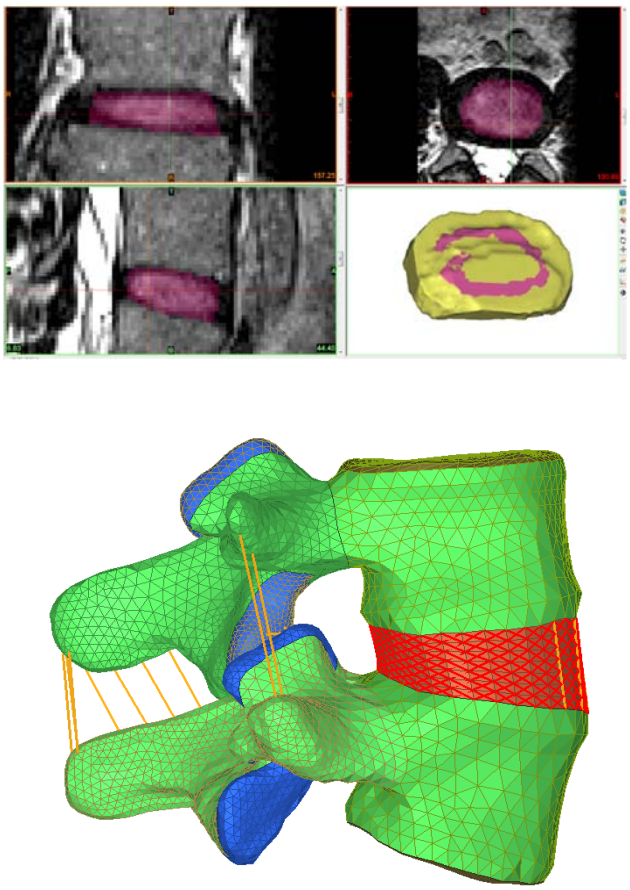

Fig. 5.1. Different steps of 3D model acquisition: (a) reconstruction of the L4-L5 nucleus and disc from MRI date, (b) FE model of the lumbar FSU L4-L5

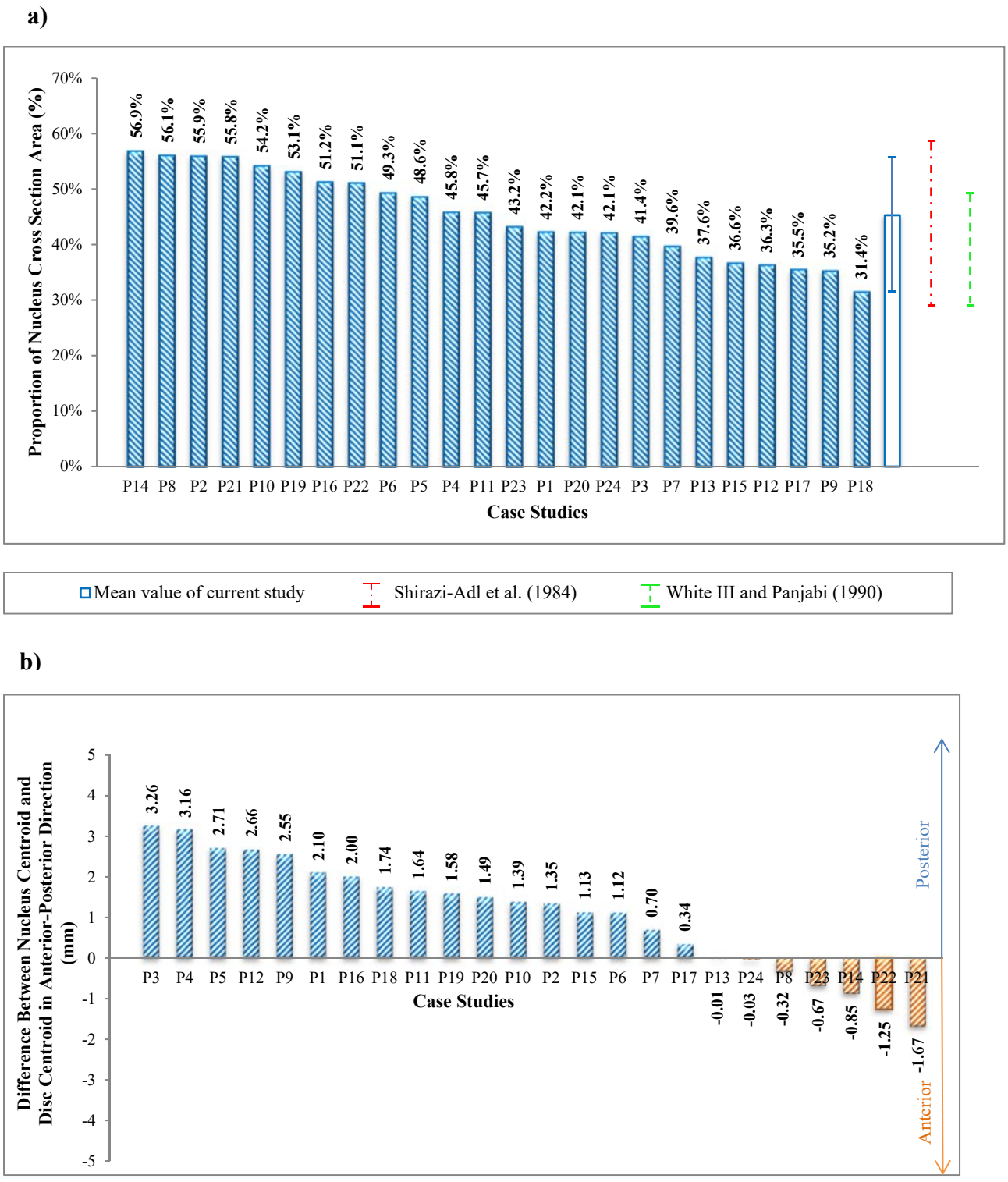

Fig. 5.2. Measurements of size and position of nucleus in respect to L4-L5 intervertebral disc for 24 individuals and the reported ranges of the size of the nucleus in literature: (a) proportion of the nucleus cross sectional area to the whole disc area (%), (b) difference between nucleus centroid and disc centroid in anterior-posterior direction(mm)

FE Model

Geometry and Mesh: Geometry of the L4 and L5 vertebrae was reconstructed using CT scans of a 20 years old male with a slice thickness of 1 mm taken from the University of Alberta Hospital data base (Naserkhaki et al., 2016b, 2017b) then meshed using the software Hypermesh (Hyperworks 14.0, Altair, USA)(Fig. 5.1b). Each vertebra included cortical bone and bony endplates meshed with 3-node shell elements of 1mm thickness as well as cancellous bone meshed with 4-node tetrahedral solid element (Naserkhaki et al. 2016a, 2016b).

The intervertebral disc was generated between the two adjacent endplates by extruding 8-node hexahedral solid elements. The proportion of the cross-sectional area of nucleus and annulus as well as the nucleus position center were changed according to the cases studied while the height and cross-sectional area of the whole disc were kept constant during all analyses. Elements of the annulus were reinforced by eight crisscross layers of annular fibers modeled using unidirectional springs. The orientation of the fibers were arranged to incline alternatively at an angle close to ±35° to the horizontal plane (El-Rich et al., 2009; Schmidt et al., 2007b; Natarajan & Andersson, 1999).

The surrounding ligaments including Anterior Longitudinal Ligament, Posterior Longitudinal Ligament, Capsular Ligament, Transvers Ligament, Supraspinous Ligament, Interspinous Ligament, and Ligamentum Flavium were simulated by one-dimensional, nonlinear unidirectional springs resisting tension only (Naserkhaki et al. 2016a, 2016b, 2017b; Breau et al., 1991). The articular joints were simulated by frictionless surface-to-surface contact between cartilaginous facets (Naserkhaki et al. 2016b, 2017b).

Material Properties: Material properties of all spinal components were derived from the literature (Table 5.2). Linear elastic materials were used for the cartilaginous endplates and bony structures including cortical bone and cancellous bone. The annulus and nucleus were modeled using incompressible, hyper-elastic Mooney-Rivlin formulation. The annular fibers were governed by nonlinear force-displacement curves developed from the stress-strain curves with stiffness increasing from inner to outer layers of the annulus. Ligaments were simulated using nonlinear force-displacement curves.

Table 5.2**.** Summary of material properties of the different tissues in the FE model

Material	Material Behavior	Mechanical Properties		References
Cortical bone	Linear elastic	E = 12,000 MPa	v = 0.30	Naserkhaki et al., 2016a, 2016b, 2017b; Schmidt et al., 2007b; Goto et al., 2003
Cancellous bone		E = 200 MPa	v = 0.315	
Cartilaginous Endplate		E= 23.8 MPa	v = 0.4	
Nucleus pulposus	Hyeper-elastic(Mooney-Rivlin)	C10 = 0.12	C01=0.030	Naserkhaki et al., 2016 a, 2016b, 2017b; El-Rich et al., 2009; Schmidt et al., 2007b
Annulus ground substance		C10 = 0.18	C01=0.045	
Annular fibers	Nonlinear stress-strain curve			Shirazi-Adl et al., 1984,1986; Schmidt et al., 2006; Naserkhaki et al., 2016a, 2016b,2017b
Ligaments	Nonlinear force displacement curve			Rohlmann et al., 2006

Validation: Model 44 has extensively been validated under different loading scenario as reported in details in Naserkhaki et al. (2017b), and its predictions were in good agreement with *in-vitro* and other numerical studies. The other models also predicted the IDP and the IVR that fell into the *in-vitro* range.

Loading and Boundary Conditions

The superior endplate and facet joints of L4 and the inferior end plate and facet joints of the L5 were constrained as two rigid bodies. The inferior endplate and facet joints of the L5 vertebra were fixed (Naserkhaki et al., 2017b; Heuer et al., 2007a, 2007b). A compressive follower load (FL) whose line of action passes through the center of each vertebra (Naserkhaki et al., 2016b; 2017b;

Shirazi-Adl, 2006; Patwardhan et al., 1999) was applied in addition to moment of fixed or variable directions applied at the L4 vertebra according to the following cases:

Case1: Pure moment of 10Nm around three anatomical axes: flexion (FLX, +ve)/extension (EXT, -ve); right lateral bending (RLB, +ve)/left lateral bending (LLB, -ve); and left axial rotation (LAR, +ve)/right axial rotation (RAR, -ve)/ (Panjabi et al., 1994)

Case2: FL of 500N combined with unconstrained moment of 10Nm around three anatomical axes (FL+FLX, FL+EXT, FL+RLB, FL+LLB, FL+LAR, FL+RAR (Heuer et al., 2007a, 2007b).

Case3: FL of 500N combined with 10Nm resulting moment whose direction varied gradually every 15^{o} from FLX or EXT to RLB (Schmidt et al., 2007b).

Case4: FL of 500N combined with 10Nm resulting moment whose direction changed gradually every 15^{o} from FLX or EXT to LAR (Schmidt et al., 2007b).

In cases 3 and 4, the resulting moment between two anatomical movement like flexion and lateral bending for instance, was always 10 Nm about an oblique spatial axis (Schmidt et al., 2007b). In total, 32 loading scenarios evaluated the intervertebral rotation (IVR), intradiscal pressure (IDP), and maximum annular fibers strain.

5.3. Results

Intervertebral rotation (IVR)

Under FL and moment (case 2), the models with large nucleus demonstrated relatively stiffer behavior during flexion and axial rotation. The IVR decreased by 6% and 7% respectively as compared to behavior of the models with the smallest nucleus. However, the differences under extension and lateral bending moment were less than 2% (Fig. 5.3a). The greatest IVR with magnitude of 6.6° was obtained in the model with the smallest nucleus under FL+FLX.

For the same loading condition (case 2), IVR increased by 8% during axial rotation when the nucleus centroid was shifted from 1.5 mm anteriorly to 3.25 mm posteriorly.

Moving the nucleus posteriorly increased IVR slightly (by 1.4%) while a negligible decrease (< 1%) was obtained when the nucleus was shifted anteriorly during flexion (Fig. 5.3b).

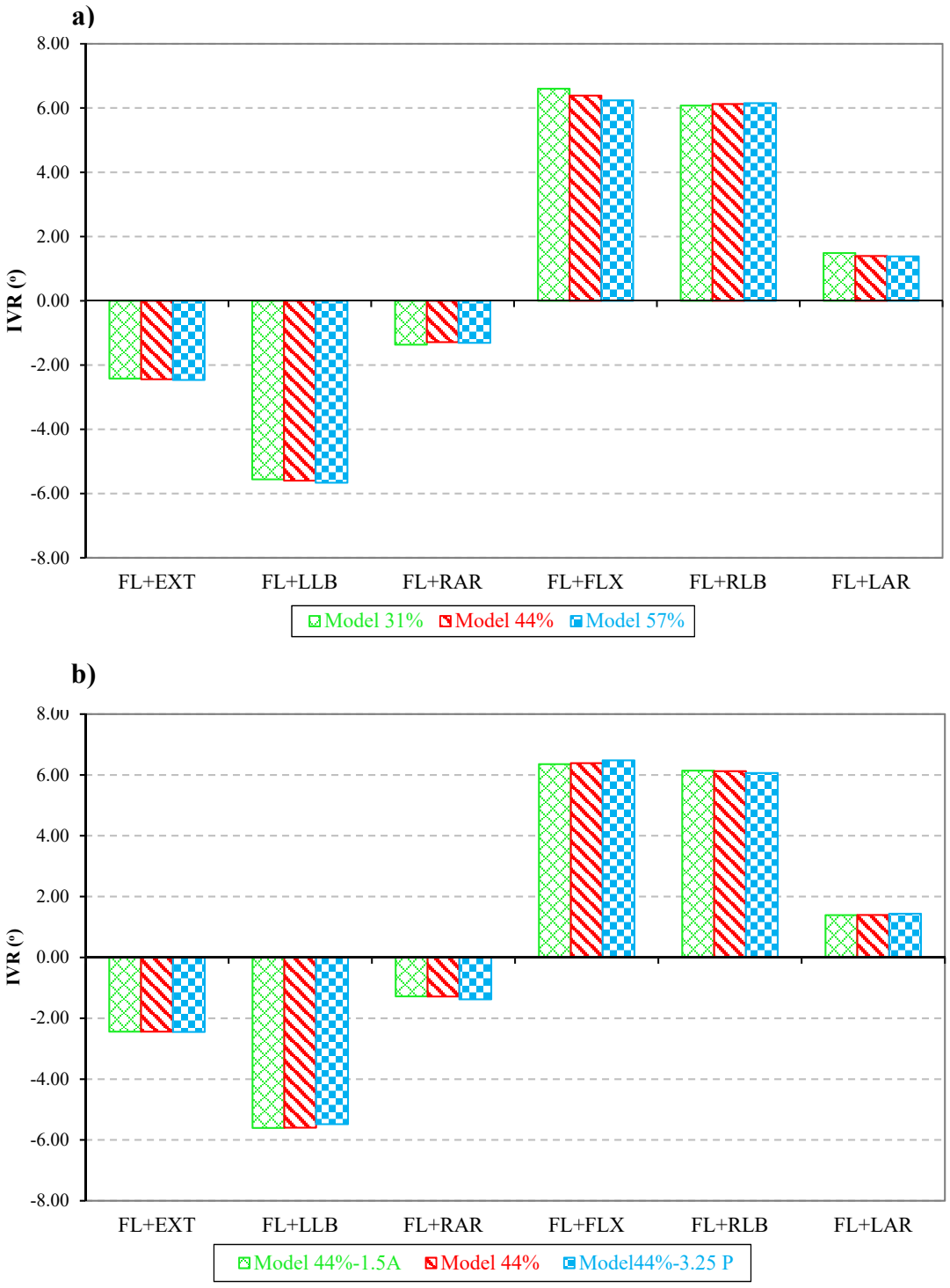

Fig. 5.3. Change of L4-L5 intervertebral rotation in combined loading scenario of 500 N follower load plus 10Nm moment in the principle planes: (a) in different sizes of nucleus, (b) in different positions of nucleus

Intradiscal pressure (IDP)

Pure moment loading (Case 1)

The highest IDP was obtained under FLX for all sizes and positions of the nucleus. IDP and size of the nucleus were inversely proportional under all pure moments around the anatomical axes (Fig. 5.4a). The highest change of IDP (51%) due to the nucleus size was obtained under RLB.

Moving the nucleus anteriorly from the disc center increased IDP under FLX, lateral bending (RLB and LLB) and axial rotation (RAR and LAR) by 5%, 3% and 6%, respectively while a 16% decrease in IDP was obtained under EXT (Fig. 5.4b). When the nucleus was positioned posteriorly from the disc center, IDP decreased by 15%, 15% and 16% under FLX, RAR, and LAR, respectively while it increased by 5% under RLB and LLB, and by 18% under EXT (Fig. 5.4b)

FL+ moment of fixed direction loading (Case2)

Under FL combined with pure moment, variation in IDP was less noticeable than under pure moments (Case1) in all cases of size and position of nucleus. The magnitude of IDP decreased slightly in the case of the large nucleus compared to Model 44. A maximum decrease of 8% was obtained under LLB. The model with the smaller nucleus predicted a drop in IDP as well under all loading cases except FL+RLB in which IDP increased by 2% (Fig. 5.4c).

Moving the nucleus anteriorly from the disc center dropped the IDP slightly under all loading cases except FL+FLX. A maximum decrease of 7% was obtained under FL+EXT while an increase of 3% was obtained under FL+FLX. When the nucleus was positioned posteriorly from the disc center, IDP dropped by 4% and 9% under FL+ LAR and FL+FLX respectively while it increased by 7% under FL+EXT and remained almost unchanged under the other loading cases (Fig. 5.4d).

FL+ moment of variable direction (Case3 and Case4)

A representative distribution of IDP as a function of the FL and moment combinations whose magnitude remained constant and direction changed from FLX/EXT to RLB and from FLX/EXT to LAR is shown in Fig. 5.5 and Fig. 5.6 using cylindrical coordinates**.** It should be noted that these figures show asymmetrical movements where the left side of the graphs shows LAR while the right side shows RLB. The IDP is presented radially and the components of the moment of variable direction are shown in the circumference. Results revealed that changes in IDP due to the size of the nucleus were greater for moments applied around the anatomical axes as compared to those

applied around oblique axes (Fig. 5.5). While IDP was inversely proportional to the nucleus size under FL+ RLB, no clear tendency was obtained for the other cases. For instance, the nucleus with the smallest size experienced highest IDP under FL+RLB, smallest IDP under FL+FLX or FL+ EXT while under FL+LAR the magnitude of IDP fell in between those of other sizes. Also, the nucleus of medium size (Model 44) experienced the highest IDP in almost all directions of moments except the ones whose moment magnitudes varied between 5Nm FLX and 8.7Nm RLB to 5Nm EXT and 8.7Nm RLB in addition to FL (Fig. 5.5).

The effects of the nucleus position on IDP are shown in Fig. 5.6. Moving the nucleus anteriorly from the disc center increased IDP for all moment directions varying from FLX to LAR and from FLX to RLB. The model with the nucleus located posteriorly with respect to the disc center had the smallest IDP in these directions. The drop of IDP due to the posterior shift of the nucleus center was more important than the increase caused by moving the nucleus anteriorly for the disc center, particularly when the moment was applied in the FLX direction. The nucleus position had reverse effects on the IDP when the moment was applied in EXT. i.e. posterior location of nucleus center increased IDP while a decease was obtained for the anterior location. No effect of the nucleus position was found under the moment applied in the RLB direction.

Annular Fibers Strain

Annular fibers of the disc with small nucleus experienced lower tensile strain than those of the disc with large nucleus under FL+FLX or FL+EXT (Fig. 5.7a). The highest strain was located in the posterior innermost layers under FL+FLX and in the anterior innermost layers under FL+EXT (Fig. 5.7b). Moving the nucleus posteriorly from the disc center increased the strain in the posterior innermost annular fibers under FL+FLX but reduced the strain in the anterior innermost fibers under FL+EXT (Fig. 5.8). When the nucleus was shifted anteriorly from the disc center, the strain in the posterior innermost fibers reduced but increased in the anterior innermost fibers under FL+FLX (Fig. 5.8b). No noticeable change was found under FL+EXT.

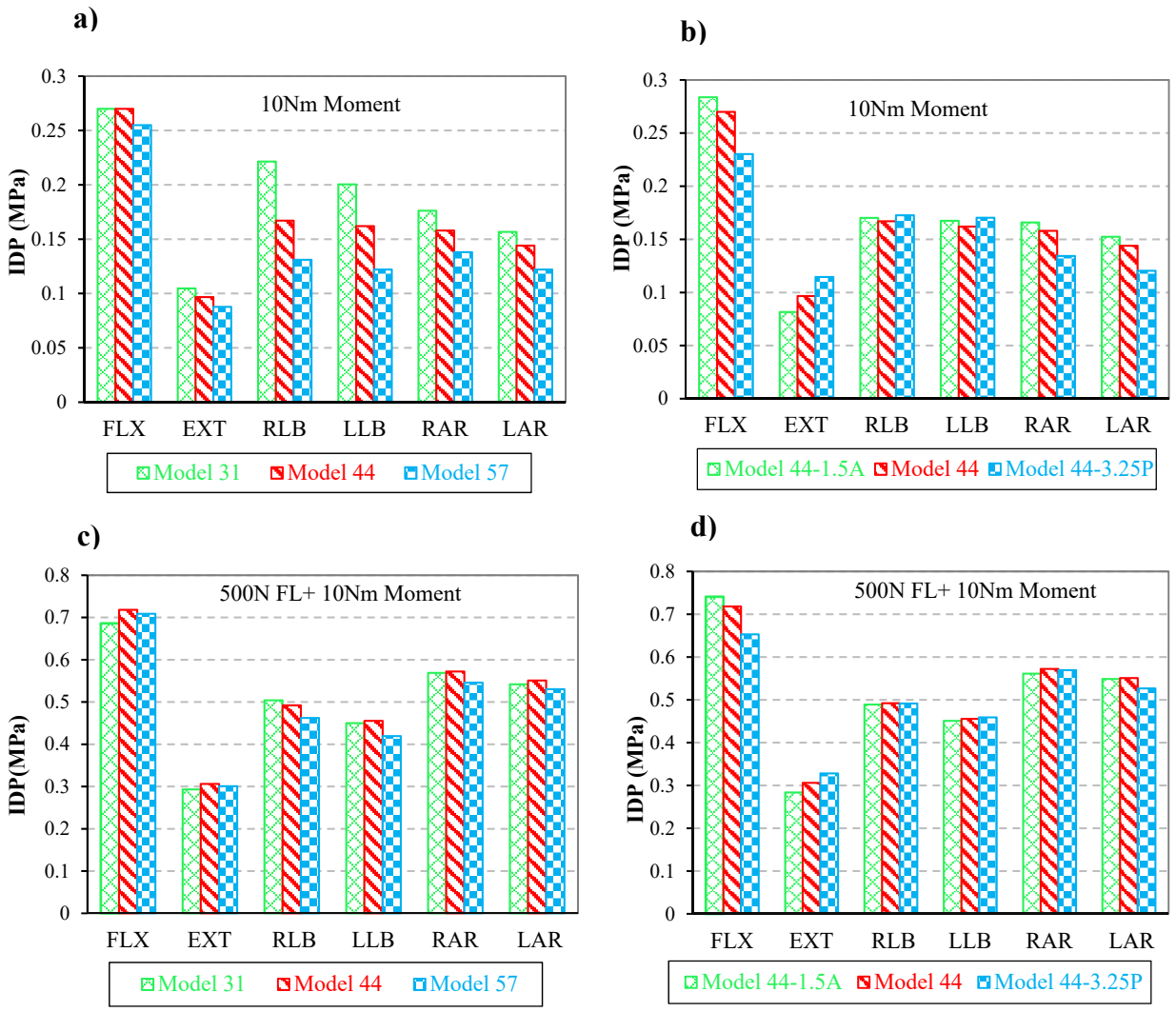

Fig. 5.4**.** IDP changes in nucleus under pure moment and combined load in: (a) different sizes of nucleus under 10Nm moment in the principle planes, (b) different positions of nucleus under 10Nm moment in the principle planes, (c) different sizes of nucleus under 500N FL plus 10Nm moment, (d) different positions of nucleus under 500N FL plus 10Nm moment

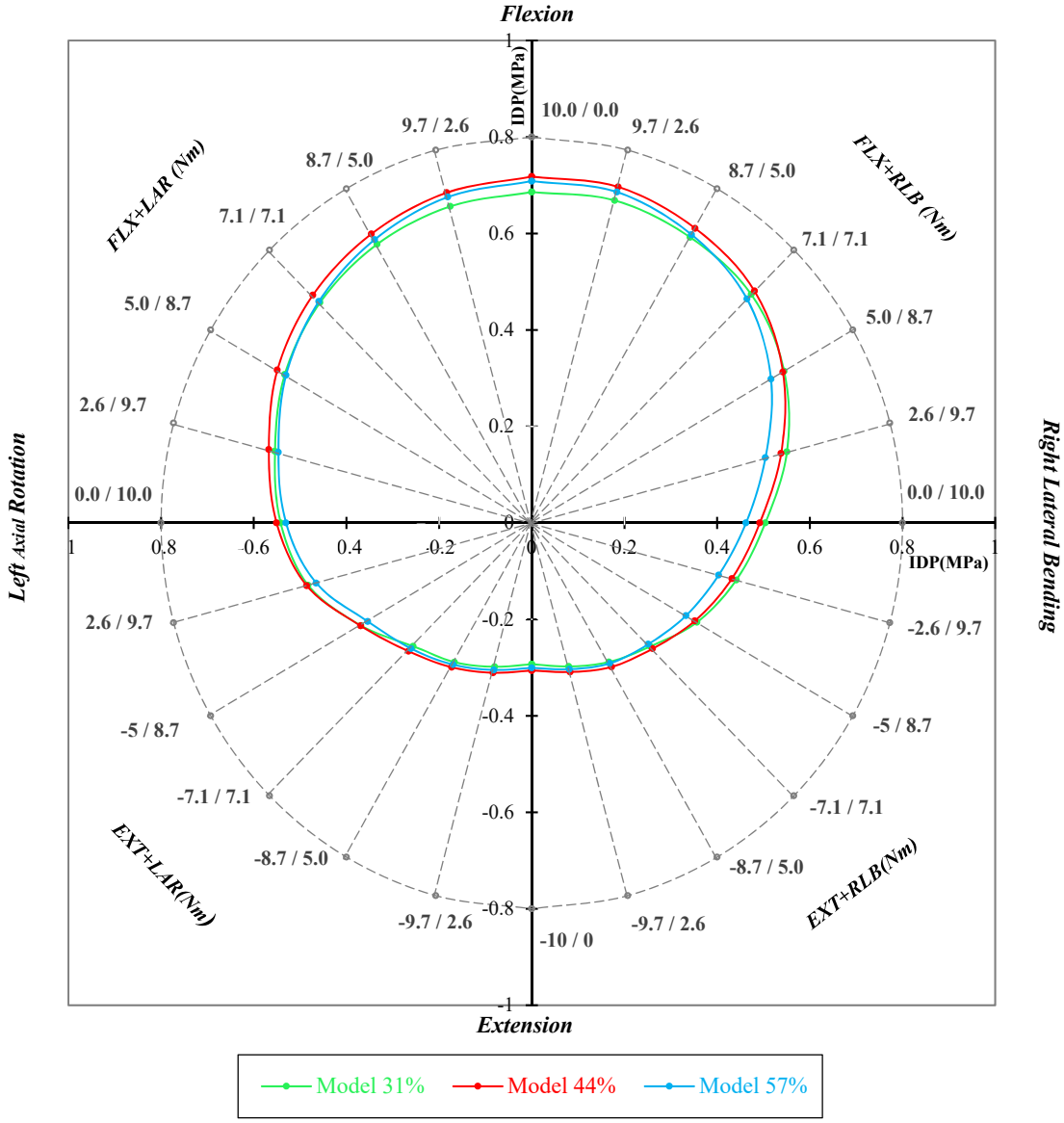

Fig. 5.5. IDP changes for different sizes of nucleus under moment of variable direction in cylindrical coordinate: IDP is presented radially and the components of the moment of variable direction are shown in the circumference. Left horizontal axis: flexion/ extension plus axial rotation; Right horizontal axis: flexion/extension plus lateral bending

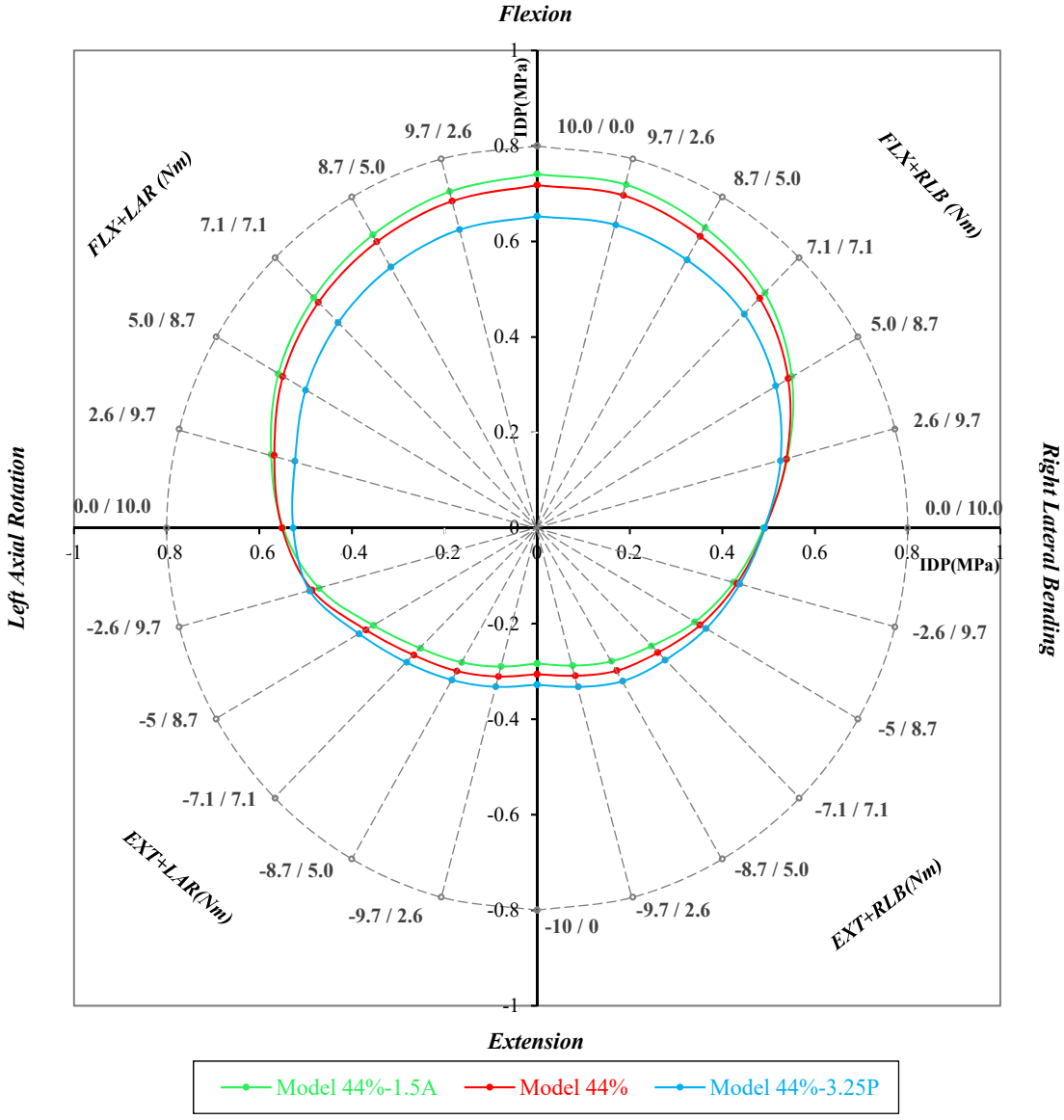

Fig. 5.6. IDP changes for different positions of nucleus under moment of variable direction in cylindrical coordinate: IDP is presented radially and the components of the moment of variable direction are shown in the circumference. Left horizontal axis: flexion/ extension plus axial rotation; Right horizontal axis: flexion/extension plus lateral bending

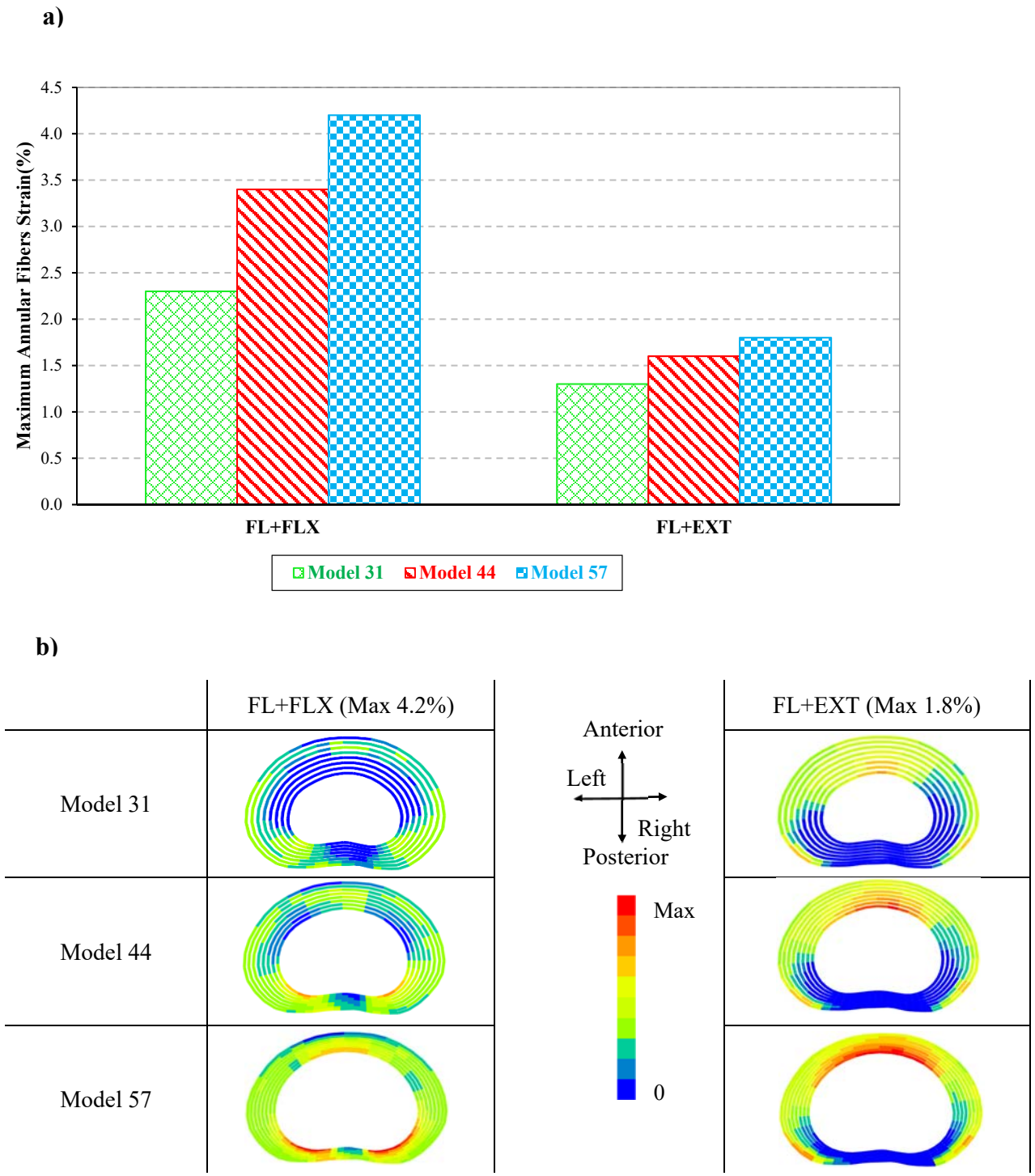

Fig. 5.7. Comparison of annular fibers strains in different sizes of nucleus under 500 FL plus 10 Nm moment in flexion/extension at level L4-L5: (a) tensile strain distribution in the annular fiber at level L4-L5, (b) maximum annular fibers strain

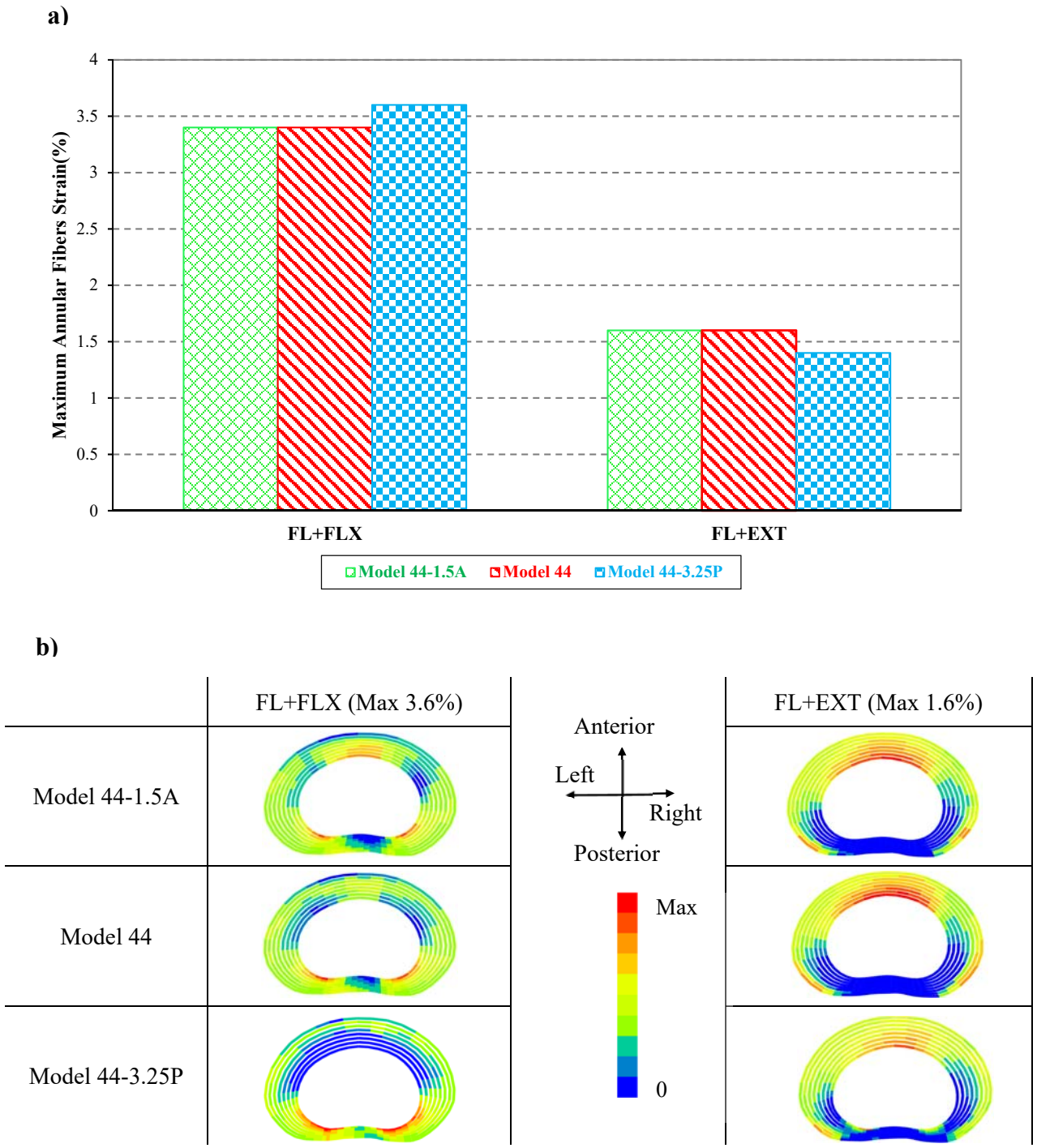

Fig. 5.8. Comparison of annular fibers strains in different positions of nucleus under 500 FL plus 10 Nm moment in flexion/extension at level L4-L5: (a) tensile strain distribution in the annular fiber, (b) maximum annular fibers strain

5.4. Discussion

Variation of the nucleus size and position in the intervertebral disc is considered as one of the factors that could affect the response of the human spine to loading (Naserkhaki et al., 2016a; Schmidt et al., 2007b). Most of the previous FE models of the lumbar FSUs or lumbar spine assumed that the nucleus occupies 44% of the total disc (Naserkhaki et al., 2016b, 2017b; El-Rich et al., 2009; Schmidt et al., 2006; Shirazi-Adl, 1994; Breau et al., 1991) with center positioned either in the disc center (Naserkhaki et al., 2016b, 2017b; El-Rich et al., 2009; Shirazi-Adl, 1994; Breau et al., 1991) or 3.5mm posteriorly from the disc center (Schmidt et al., 2006). The present study first quantified the size and position of the nucleus of L4-L5 discs of 24 subjects and investigated the effects of inter-individual nucleus cross-sectional area and position variation on the biomechanical response of the L4-L5 FSU to various loading scenarios using a validated 3D nonlinear FE model.

Nucleus size and position measures

The ratios of the nucleus to disc cross-sectional areas found in this study fell within the ranges reported by Shirazi-Adl et al. (1984). Their range however, was wider than the one reported in the literature (White III & Panjabi, 1990; Markolf & Morris, 1974; Nachemson, 1960). In agreement with previous findings (O'Connell et al., 2007; Schmidt et al., 2006), our results revealed that the nucleus cross-sectional area varies among individuals and the nucleus is not always in the disc center. The cross-sectional area reported here was determined using Geomagic software. It is the average plane between two adjacent endplates (mid-height of the disc) which is trimmed by the inner and outer lamella of the annulus. Centroid of the selected area is the average of the points on that area.

FE modeling

The current study focused only on the effects of the nucleus size and position on the mechanical response of L4-L5. To limit the several geometrical variables of the model to only the nucleus size and position with respect the disc, a single geometry and one set of material properties taken from the literature were used for all spinal structures except the annular fibers. The overall volume of annular fibers was assumed to occupy 16% of the annulus volume (Naserkhaki et al., 2016b,

2017b; Shirazi-Adl et al., 1984) and their material properties were modified according to change of annulus volume which was affected by the nucleus size and position. It should be noted that, the stiffness of the annular fibers was proportional to the annulus size i.e. increased in the discs with small nucleus. The number of annular fibers layers was kept unchanged in all models and all models were subjected to similar loading and boundary conditions. Thus, inter-individual variation of these parameters was ignored. In the validation study of Model 44, the contribution of each ligament in moment-sharing was studied under pure moment. Based on the reported results, SSL was the most load bearing ligament by resisting about 27% of the total applied flexion moment while PLL had negligible contribution (under 2%). Resistance of all ligaments together to flexion was about 45% of the total moment and the rest of the moment was resisted by disc and facets. In extension, ALL and CL ligaments resisted together about 27% of the total applied moment (Naserkhaki et al., 2017b). In addition, the contribution of the ligaments in Model 44 was also calculated under FL+ FLX and FL+EXT in the current study and the resistance of all ligaments together was about 72% and 47% respectively. Although six ligaments of ALL, CL, LF, ISL, SSL and ITL carried an important portion of the external loading especially in FL+FLX and FL+EXT, PLL had negligible contributions. Various loading scenarios including pure moment of fixed direction around the anatomical axes combined or not with FL (Naserkhaki et al., 2016b, 2017b; Heuer et al., 2007a, 2007b) as well as moments of variable direction around oblique spatial axes combined with FL simulating more complex loading (Schmidt et al., 2007b) were used. Nevertheless, these loading scenarios were only used as an approximation of *in-vivo* loading which includes gravity, muscle forces, intra-abdominal pressure, and ligaments pretensioning (Naserkhaki et al., 2016a; Rohlmann et al., 2009a, 2009b; Arjmand & Shirazi-Adl, 2006; El-Rich et al., 2004;) and is affected by the spine posture (Dreischarf et al., 2016; Arjmand & Shirazi-Adl, 2005 ; Dolan & Adams, 2001). Due to asymmetry of the FSU the FL did not pass through the exact center of the disc which produced slight rotation in addition to compression of the disc.

Nucleus size and position effects

Overall, the size and position of the nucleus had slight effects on IVR under FL+ moments in various directions. The greatest change in IVR due to nucleus size variation did not exceed 7%. The nucleus size and IVR were inversely proportional under FLX, LAR, and RAR. However, a small change with indistinct trend was obtained under EXT and RLB. This could be due in part to

the facet joints which resist EXT (Naserkhaki et al., 2016b). In general, the flexibility of the FSU decreased when the proportion of the nucleus cross-sectional area was increased. Meijer et al. (2011) also reported negligible effect on the stiffness of the FSU after changing the size of the nucleus between 30% and 50% of the disc during 10 Nm pure moment. IDP was however noticeably influenced by nucleus size particularly under pure moments and its magnitude was inversely proportional to nucleus size. The greatest change was found under RLB. Adding FL to moment reduced this effect in all loading cases which makes the hypothesis that IDP is inversely proportional to nucleus size questionable. It should be highlighted that IDP was mainly produced by the FL during the FL+moment loading cases (Naserkhaki and El-Rich, 2017a; Rohlmann et al., 2009b) and the effect of FL on the IDP was more important than the effect of the moment. As the line of action of the FL passed through the centroids of the vertebral bodies of L4 and L5, this latter was not affected by the nucleus size or position. Thus, applying more realistic (*in-vivo*) load (Liu et al., 2017) and including the fluid phase in disc modeling (Natarajan & Andersson, 2004) is expected to reveal more significant effects. In both FL+FLX and FL+EXT cases, the nucleus size and the tensile strains were directly proportional. This could be explained by the position of the annular fibers which are located farther away from the disc center in the case of the large nucleus. During FL+FLX, high tensile strains were found mostly in the innermost layer of posterolateral area, similar to previous findings (Naserkhaki et al., 2016b; Schmidt et al., 2007b; Shirazi-Adl., 1989) and were expanded to the outer lamella when the nucleus cross-sectional area was increased. Therefore, increasing the size of the nucleus could increase the possibility of the fiber failure in the posterior region during FL+FLX. In the FL+EXT moment case, highest tensile strains were located in the innermost layer of the anterolateral area (Naserkhaki et al., 2016b; Shirazi-Adl., 1989) and also in the outermost lamella of the posterolateral region (Naserkhaki et al., 2016b).

Overall, the position of the nucleus had more effects on IDP than IVR. These effects were more noticeable under pure moments as compared to FL + moments similar to the results of nucleus size. Also, applying FL+ moment of variable direction did not reveal more important variation of IDP than the one found under FL+ moment around the anatomical axes.

Maximum strain location and magnitude in the annular fibers was sensitive to position and size of the nucleus.

5.5. Conclusion

The position and size of the nucleus significantly affected the IDP under pure moments. Adding FL attenuated these effects on IDP. Under load case of FL+ moment, the annular fibers strain was influenced by these geometrical variations, especially by change of the size of the nucleus. The greater annular fibers strain was observed in the disc with larger nucleus during FL+FLX and FL+EXT. However, the IVR was slightly influenced by the size and position variation of the nucleus. In general, The FSU demonstrated stiffer behaviour when the proportion of the nucleus cross-sectional area was increased or when the position of the nucleus was shifted from the posterior side to the anterior side. It is speculated that including the fluid phase in disc modeling, analyzing the whole lumbar spine, and applying *in-vivo* loading would reveal more remarkable effects.

Conflict of interest statement

The Authors have no conflict of interest to declare.

Acknowledgements

This study was supported by NSERC Discovery Grant (402046-2013), Canada.

We thank Dr. Jacob L. Jaremko, Associate Professor, Department of Radiology & Diagnostic Imaging, University of Alberta, for providing CT scans and MR images that greatly assisted the measurements of disc geometry and FE modeling.

References

Arjmand, N., & Shirazi-Adl, A. (2006). Model and in vivo studies on human trunk load partitioning and stability in isometric forward flexions. Journal of biomechanics, 39(3), 510-521.

Arjmand, N., & Shirazi-Adl, A. (2005). Biomechanics of changes in lumbar posture in static lifting. Spine, 30(23), 2637-2648.

Breau, C., Shirazi-Adl, A., & De Guise, J. (1991). Reconstruction of a human ligamentous lumbar spine using CT images—a three-dimensional finite element mesh generation. Annals of biomedical engineering, 19(3), 291-302.

Campana, S., Guise, J. A., Rillardon, L., Mitton, D., & Skalli, W. (2007). Lumbar intervertebral disc mobility: Effect of disc degradation and of geometry. European Journal of Orthopaedic Surgery & Traumatology, 17(6), 533. doi:10.1007/s00590-007-0243-z

Dolan, P., & Adams, M. A. (2001). Recent advances in lumbar spinal mechanics and their significance for modelling. Clinical Biomechanics, 16, S8-S16.

Dreischarf, M., Shirazi-Adl, A., Arjmand, N., Rohlmann, A., & Schmidt, H. (2016). Estimation of loads on human lumbar spine: a review of in vivo and computational model studies. Journal of biomechanics, 49(6), 833-845.

El-Rich, M., Arnoux, P. J., Wagnac, E., Brunet, C., & Aubin, C. E. (2009). Finite element investigation of the loading rate effect on the spinal load-sharing changes under impact conditions. Journal of biomechanics, 42(9), 1252-1262.

El-Rich, M., Shirazi-Adl, A., & Arjmand, N. (2004). Muscle activity, internal loads, and stability of the human spine in standing postures: combined model and in vivo studies. Spine, 29(23), 2633-2642.

Goto, K., Tajima, N., Chosa, E., Totoribe, K., Kubo, S., Kuroki, H., & Arai, T. (2003). Effects of lumbar spinal fusion on the other lumbar intervertebral levels (three-dimensional finite element analysis). Journal of Orthopaedic Science, 8(4), 577-584.

Heuer, F., Schmidt, H., Klezl, Z., Claes, L., & Wilke, H. J. (2007a). Stepwise reduction of functional spinal structures increase range of motion and change lordosis angle. Journal of biomechanics, 40(2), 271-280

Heuer, F., Schmidt, H., Claes, L., & Wilke, H. J. (2007b). Stepwise reduction of functional spinal structures increase vertebral translation and intradiscal pressure. Journal of biomechanics, 40(4), 795-803.

Jacobs, N. T., Cortes, D. H., Peloquin, J. M., Vresilovic, E. J., & Elliott, D. M. (2014). Validation and application of an intervertebral disc finite element model utilizing independently constructed tissue-level constitutive formulations that are nonlinear, anisotropic, and time-dependent. Journal of biomechanics, 47(11), 2540-2546.

Markolf, K. L., & Morris, J. M. (1974). The Structural Components of the Intervertebral Disc: A study of their contributions to the ability of the disc to withstand compressive forces. JBJS, 56(4), 675-687.

Meijer, G. J., Homminga, J., Veldhuizen, A. G., & Verkerke, G. J. (2011). Influence of interpersonal geometrical variation on spinal motion segment stiffness: implications for patient-specific modeling. Spine, 36(14), E929-E935.

Nachemson, A. L., Schultz, A. B., & Berkson, M. H. (1979). Mechanical properties of human lumbar spine motion segments: Influences of age, sex, disc level, and degeneration. Spine, 4(1), 1-8.

Nachemson, A. (1960). Lumbar intradiscal pressure: experimental studies on post-mortem material. Acta Orthopaedica Scandinavica, 31(sup43), 1-104.

Naserkhaki, S., & El-Rich, M. (2017a). Sensitivity of lumbar spine response to follower load and flexion moment: finite element study. Computer methods in biomechanics and biomedical engineering, 20(5), 550-557.

Naserkhaki, S., Arjmand, N., Shirazi-Adl, A., Farahmand, F., & El-Rich, M. (2017b). Effects of eight different ligament property datasets on biomechanics of a lumbar L4-L5 finite element model. Journal of Biomechanics.

Naserkhaki, S., Jaremko, J. L., & El-Rich, M. (2016a). Effects of inter-individual lumbar spine geometry variation on load-sharing: Geometrically personalized finite element study. Journal of Biomechanics, 49(13), 2909-2917.

Naserkhaki, S., Jaremko, J. L., Adeeb, S., & El-Rich, M. (2016b). On the load-sharing along the ligamentous lumbosacral spine in flexed and extended postures: Finite element study. Journal of biomechanics, 49(6), 974-982.

Natarajan, R. N., Williams, J. R., & Andersson, G. B. (2004). Recent advances in analytical modeling of lumbar disc degeneration. Spine, 29(23), 2733-2741.

Natarajan, R. N., & Andersson, G. B. (1999). The influence of lumbar disc height and cross-sectional area on the mechanical response of the disc to physiologic loading. Spine, 24(18), 1873.

Noailly, J., Wilke, H. J., Planell, J. A., & Lacroix, D. (2007). How does the geometry affect the internal biomechanics of a lumbar spine bi-segment finite element model? Consequences on the validation process. Journal of biomechanics, 40(11), 2414-2425.

O'Connell, G. D., Vresilovic, E. J., & Elliott, D. M. (2007). Comparison of animals used in disc research to human lumbar disc geometry. Spine, 32(3), 328-333.

Panjabi, M.M., Oxland, TR., Yamamoto I., & Crisco, JJ. (1994). Mechanical behavior of the human lumbar and lumbosacral spine as shown by three-dimensional load-displacement curves. The Journal of Bone & Joint Surgery, 76(3), 413-424. doi:10.2106/00004623-199403000-00012

Patwardhan, A. G., Havey, R. M., Meade, K. P., Lee, B., & Dunlap, B. (1999). A Follower Load Increases the Load-Carrying Capacity of the Lumbar Spine in Compression. Spine, 24(10), 1003-1009.

Pooni, J. S., Hukins, D. W., Harris, P. F., Hilton, R. C., & Davies, K. E. (1986). Comparison of the structure of human intervertebral discs in the cervical, thoracic and lumbar regions of the spine. Surgical and Radiologic Anatomy : SRA, 8(3), 175-182. doi:10.1007/BF02427846

Rohlmann, A., Zander, T., Rao, M., & Bergmann, G. (2009a). Realistic loading conditions for upper body bending. Journal of Biomechanics, 42(7), 884-890.

Rohlmann, A., Zander, T., Rao, M., & Bergmann, G. (2009b). Applying a follower load delivers realistic results for simulating standing. Journal of biomechanics, 42(10), 1520-1526.

Rohlmann, A., Bauer, L., Zander, T., Bergmann, G., & Wilke, H. J. (2006). Determination of trunk muscle forces for flexion and extension by using a validated finite element model of the lumbar spine and measured in vivo data. Journal of Biomechanics, 39(6), 981-989.

Schmidt, H., Kettler, A., Rohlmann, A., Claes, L., & Wilke, H. J. (2007a). The risk of disc prolapses with complex loading in different degrees of disc degeneration–a finite element analysis. Clinical Biomechanics, 22(9), 988-998.

Schmidt, H., Kettler, A., Heuer, F., Simon, U., Claes, L., & Wilke, H. J. (2007b). Intradiscal pressure, shear strain, and fiber strain in the intervertebral disc under combined loading. Spine, 32(7), 748-755

Schmidt, H., Heuer, F., Simon, U., Kettler, A., Rohlmann, A., Claes, L., & Wilke, H. J. (2006). Application of a new calibration method for a three-dimensional finite element model of a human lumbar annulus fibrosus. Clinical Biomechanics, 21(4), 337-344.

Shirazi-Adl, A. (2006). Analysis of large compression loads on lumbar spine in flexion and in torsion using a novel wrapping element. Journal of biomechanics, 39(2), 267-275.

Shirazi-Adl, A. (1994). Biomechanics of the lumbar spine in sagittal/lateral moments. Spine, 19(21), 2407-2414.

Shiraz-Adl, A. (1989). Strain in Fibers of a Lumbar Disc: Analysis of the Role of Lifting in Producing Disc Prolapse. Spine, 14(1), 96-103.

Shirazi-Adl, A. A. A. S. S., Ahmed, A. M., & Shrivastava, S. C. (1986). Mechanical response of a lumbar motion segment in axial torque alone and combined with compression. Spine, 11(9), 914-927.

Shirazi-adl, S. A., Shrivastava, S. C., & Ahmed, A. M. (1984). Stress Analysis of the Lumbar Disc-Body Unit in Compression A Three-Dimensional Nonlinear Finite Element Study. Spine, 9(2), 120-134.

White III, A.A., Panjabi, M.M.(1990). Clinical Biomechanics of the Spine, second ed. Lippincott Williams & Wilkins.

Chapter 6: Summary and Conclusions

6.1. Summary

This study aimed to:

1. Determine the size and position of the nucleus with respect to the disc at the lumbar level L4-L5 of 24 individuals using their MRI data
2. Investigate the effects of the size and position of the nucleus on the mechanical response of the FSU L4-L5 to various load combinations using the FE method.

The 3D geometries of the L4-L5 intervertebral discs of 24 individuals were reconstructed using their MR images. The cross-sectional area of the nucleus and the whole disc as well as the position of the nucleus center with respect to the whole disc center in the anterior-posterior direction were measured. The range of the size and position of nucleus with respect to the L4-L5 disc was obtained and compared to the literature. The obtained values fell within the ranges reported in the literature.

Four 3D nonlinear FE models of the FSU L4-L5 with distinct sizes and positions of the nucleus with respect to the disc were created according to the obtained results. Also, one additional model with the nucleus size proportion of 44% and center located in the center of the disc was modeled according to previous histological findings and FE studies. This model has recently been validated under various loading scenarios against experimental studies. The RoM, IDP, and the axial strains in the ligaments all fell within the *in-vitro* ranges.

The models were subjected to the 32 different loading scenarios including FL combined or not with moments with variable directions to investigate the effects of the nucleus size and position variation on the mechanical response of the FSU L4-L5. The IVR, IDP, and maximum annular fibers strain were compared.

6.2. Conclusion

6.2.1 Intervertebral disc measurements (Objective 1, Chapter 3)

The current study revealed that the proportion of the nucleus cross-sectional area to the whole disc varied from 31% to 57%, and the location of the nucleus center varied between 1.67 mm anteriorly to 3.26 mm posteriorly with respect to the center of the whole disc. Furthermore, poor correlation was obtained between the nucleus size and position while no correlation was found between the nucleus size and age and between the nucleus position and age.

6.2.2 Effects of nucleus size and position on response of the Lumbar FSU L4-L5 to complex loading (Objective 2, Chapter 4 & Chapter 5)

The position and size of the nucleus noticeably affected the IDP in the nucleus under pure moment. The IDP and the size of the nucleus were inversely proportional under all pure moments around the anatomical axes. The highest change of IDP (51%) due to the nucleus size was obtained under lateral bending. The IDP decreased in FLX, LAR, and RAR and increased in EXT as the center of the nucleus was shifted from anterior to the posterior side of the disc center. Adding FL attenuated these effects on the IDP in all cases which makes the hypothesis that IDP is inversely proportional to nucleus size questionable. Maximum strain location and magnitude in the annular fibers was sensitive to the position and size of the nucleus, especially to the change of the size of the nucleus. The greater annular fibers strain was observed in the disc with larger nucleus during FL+FLX and FL+EXT. However, the IVR was slightly influenced by the size and position variation of the nucleus. In general, The FSU demonstrated stiffer behaviour when the proportion of the nucleus cross-sectional area was increased or when the position of the nucleus was shifted from the posterior side to the anterior side. It is speculated that including the fluid phase in disc modeling, analyzing the whole lumbar spine, and applying *in-vivo* loading would reveal more remarkable effects.

6.3. Recommendations for the future research

Some suggestions that could be considered for further work are discussed below:

- Studying effects of nucleus size and position under *in-vivo* loads which include muscle forces and ligament pretensioning
- Analyzing the whole lumbar spine
- Including the fluid phase in disc modeling
- Using personalized geometry of the vertebrae

Bibliography

Adams, M. A. (2015). Intervertebral Disc Tissues. In Mechanical Properties of Aging Soft Tissues (pp. 7-35). Springer International Publishing.

Adams, M. A., Dolan, P., Hutton, W. C., & Porter, R. W. (1990). Diurnal changes in spinal mechanics and their clinical significance. Bone & Joint Journal, 72(2), 266-270.

Amonoo-Kuofi, H. S. (1991). Morphometric changes in the heights and anteroposterior diameters of the lumbar intervertebral discs with age. Journal of anatomy, 175, 159.

Andersson, G. B., & Schultz, A. B. (1979). Effects of fluid injection on mechanical properties of intervertebral discs. Journal of biomechanics, 12(6), 453-458.

Arjmand, N., & Shirazi-Adl, A. (2006). Model and in vivo studies on human trunk load partitioning and stability in isometric forward flexions. Journal of biomechanics, 39(3), 510-521.

Arjmand, N., & Shirazi-Adl, A. (2005). Biomechanics of changes in lumbar posture in static lifting. Spine, 30(23), 2637-2648.

Beneck, G. J., Kulig, K., Landel, R. F., & Powers, C. M. (2005). The relationship between lumbar segmental motion and pain response produced by a posterior-to-anterior force in persons with nonspecific low back pain. Journal of Orthopaedic & Sports Physical Therapy, 35(4), 203-209.

Benzel, E. C. (Ed.). (2011). Biomechanics of spine stabilization. Thieme.

Bigos, S., Bowyer, O., Braen, G., Brown, K., Deyo, R., Haldeman, S., Hart, J.L., Johnson, E.W., Keller, R., Kido, D. & Liang, M. H. (1994). Acute lower back problems in adults. Rockville, MD: Agency for Health Care Policy and Research.

Bogduk, N. (2005). Clinical anatomy of the lumbar spine and sacrum. Elsevier Health Sciences.

Breau, C., Shirazi-Adl, A., & De Guise, J. (1991). Reconstruction of a human ligamentous lumbar spine using CT images—a three-dimensional finite element mesh generation. Annals of biomedical engineering, 19(3), 291-302.

Campana, S., Guise, J. A., Rillardon, L., Mitton, D., & Skalli, W. (2007). Lumbar intervertebral disc mobility: Effect of disc degradation and of geometry. European Journal of Orthopaedic Surgery & Traumatology, 17(6), 533. doi:10.1007/s00590-007-0243-z

Chazal, J., Tanguy, A., Bourges, M., Gaurel, G., Escande, G., Guillot, M., & Vanneuville, G. (1985). Biomechanical properties of spinal ligaments and a histological study of the supraspinal ligament in traction. Journal of biomechanics, 18(3), 167-176.

Cholewicki, J., & McGill, S. M. (1996). Mechanical stability of the in vivo lumbar spine: implications for injury and chronic low back pain. Clinical biomechanics, 11(1), 1-15.

Dolan, P., & Adams, M. A. (2001). Recent advances in lumbar spinal mechanics and their significance for modelling. Clinical Biomechanics, 16, S8-S16.

Dreischarf, M., Shirazi-Adl, A., Arjmand, N., Rohlmann, A., & Schmidt, H. (2016). Estimation of loads on human lumbar spine: a review of in vivo and computational model studies. Journal of biomechanics, 49(6), 833-845.

El-Rich, M., Arnoux, P. J., Wagnac, E., Brunet, C., & Aubin, C. E. (2009). Finite element investigation of the loading rate effect on the spinal load-sharing changes under impact conditions. Journal of biomechanics, 42(9), 1252-1262.

El-Rich, M., Shirazi-Adl, A., & Arjmand, N. (2004). Muscle activity, internal loads, and stability of the human spine in standing postures: combined model and in vivo studies. Spine, 29(23), 2633-2642.

Goto, K., Tajima, N., Chosa, E., Totoribe, K., Kubo, S., Kuroki, H., & Arai, T. (2003). Effects of lumbar spinal fusion on the other lumbar intervertebral levels (three-dimensional finite element analysis). Journal of Orthopaedic Science, 8(4), 577-584.

Heuer, F., Schmidt, H., Klezl, Z., Claes, L., & Wilke, H. J. (2007a). Stepwise reduction of functional spinal structures increase range of motion and change lordosis angle. Journal of biomechanics, 40(2), 271-280

Heuer, F., Schmidt, H., Claes, L., & Wilke, H. J. (2007b). Stepwise reduction of functional spinal structures increase vertebral translation and intradiscal pressure. Journal of biomechanics, 40(4), 795-803.

Hickey, D.S., & Hukins, D.W.L (1980). Relation between the structure of the annulus fibrosus and the function and failure of the intervertebral disc. Spine, 5(2), 106-116.

Jacobs, N. T., Cortes, D. H., Peloquin, J. M., Vresilovic, E. J., & Elliott, D. M. (2014). Validation and application of an intervertebral disc finite element model utilizing independently

constructed tissue-level constitutive formulations that are nonlinear, anisotropic, and time-dependent. Journal of biomechanics, 47(11), 2540-2546.

Kirkaldy-Willis, W. H., & Farfan, H. F. (1982). Instability of the lumbar spine. Clinical orthopaedics and related research, 165, 110-123.

Koeller, W., Muehlhaus, S., Meier, W., & Hartmann, F. (1986). Biomechanical properties of human intervertebral discs subjected to axial dynamic compression—influence of age and degeneration. Journal of Biomechanics, 19(10), 807-816.

Lundon, K., & Bolton, K. (2001). Structure and function of the lumbar intervertebral disk in health, aging, and pathologic conditions. Journal of Orthopaedic & Sports Physical Therapy, 31(6), 291-306.

Markolf, K. L., & Morris, J. M. (1974). The Structural Components of the Intervertebral Disc: A study of their contributions to the ability of the disc to withstand compressive forces. JBJS, 56(4), 675-687.

McGill, S. M. (2015). Low Back Disorders, 3E. Human Kinetics.

Meijer, G. J., Homminga, J., Veldhuizen, A. G., & Verkerke, G. J. (2011). Influence of interpersonal geometrical variation on spinal motion segment stiffness: implications for patient-specific modeling. Spine, 36(14), E929-E935.

Middleditch, A., & Oliver, J. (2005). Functional anatomy of the spine. Elsevier Health Sciences.

Myklebust, J. B., Pintar, F., Yoganandan, N., Cusick, J. F., Maiman, D., Myers, T. J., & Sances Jr, A. (1988). Tensile strength of spinal ligaments. Spine, 13(5), 528-531.

Nachemson, A. L., Schultz, A. B., & Berkson, M. H. (1979). Mechanical properties of human lumbar spine motion segments: Influences of age, sex, disc level, and degeneration. Spine, 4(1), 1-8.

Nachemson, A. (1960). Lumbar intradiscal pressure: experimental studies on post-mortem material. Acta Orthopaedica Scandinavica, 31(sup43), 1-104.

Naserkhaki, S., & El-Rich, M. (2017a). Sensitivity of lumbar spine response to follower load and flexion moment: finite element study. Computer methods in biomechanics and biomedical engineering, 20(5), 550-557.

Naserkhaki, S., Arjmand, N., Shirazi-Adl, A., Farahmand, F., & El-Rich, M. (2017b). Effects of eight different ligament property datasets on biomechanics of a lumbar L4-L5 finite element model. Journal of Biomechanics.

Naserkhaki, S., Jaremko, J. L., & El-Rich, M. (2016a). Effects of inter-individual lumbar spine geometry variation on load-sharing: Geometrically personalized finite element study. Journal of Biomechanics, 49(13), 2909-2917.

Naserkhaki, S., Jaremko, J. L., Adeeb, S., & El-Rich, M. (2016b). On the load-sharing along the ligamentous lumbosacral spine in flexed and extended postures: Finite element study. Journal of biomechanics, 49(6), 974-982.

Natarajan, R. N., Williams, J. R., & Andersson, G. B. (2004). Recent advances in analytical modeling of lumbar disc degeneration. Spine, 29(23), 2733-2741.

Natarajan, R. N., & Andersson, G. B. (1999). The influence of lumbar disc height and cross-sectional area on the mechanical response of the disc to physiologic loading. Spine, 24(18), 1873.

Noailly, J., Wilke, H. J., Planell, J. A., & Lacroix, D. (2007). How does the geometry affect the internal biomechanics of a lumbar spine bi-segment finite element model? Consequences on the validation process. Journal of biomechanics, 40(11), 2414-2425.

O'Connell, G. D., Vresilovic, E. J., & Elliott, D. M. (2007). Comparison of animals used in disc research to human lumbar disc geometry. Spine, 32(3), 328-333.

Panjabi, M.M., Oxland, TR., Yamamoto I., & Crisco, JJ. (1994). Mechanical behavior of the human lumbar and lumbosacral spine as shown by three-dimensional load-displacement curves. The Journal of Bone & Joint Surgery, 76(3), 413-424. doi:10.2106/00004623-199403000-00012

Panjabi, M. M., Goel, V. K., & Takata, K. (1982). Physiologic Strains in the Lumbar Spinal Ligaments: An In VitroBiomechanical Study. Spine, 7(3), 192-203.

Patwardhan, A. G., Havey, R. M., Meade, K. P., Lee, B., & Dunlap, B. (1999). A Follower Load Increases the Load-Carrying Capacity of the Lumbar Spine in Compression. Spine, 24(10), 1003-1009.

Pintar, F. A., Yoganandan, N., Myers, T., Elhagediab, A., & Sances, A. (1992). Biomechanical properties of human lumbar spine ligaments. Journal of biomechanics, 25(11), 1351-1356.

Pooni, J. S., Hukins, D. W., Harris, P. F., Hilton, R. C., & Davies, K. E. (1986). Comparison of the structure of human intervertebral discs in the cervical, thoracic and lumbar regions of the spine. Surgical and Radiologic Anatomy : SRA, 8(3), 175-182. doi:10.1007/BF02427846

Raj, P. P. (2008). Intervertebral Disc: Anatomy-Physiology-Pathophysiology-Treatment. Pain Practice, 8(1), 18-44.

Rohlmann, A., Zander, T., Rao, M., & Bergmann, G. (2009a). Realistic loading conditions for upper body bending. Journal of Biomechanics, 42(7), 884-890.

Rohlmann, A., Zander, T., Rao, M., & Bergmann, G. (2009b). Applying a follower load delivers realistic results for simulating standing. Journal of biomechanics, 42(10), 1520-1526.

Rohlmann, A., Bauer, L., Zander, T., Bergmann, G., & Wilke, H. J. (2006). Determination of trunk muscle forces for flexion and extension by using a validated finite element model of the lumbar spine and measured in vivo data. Journal of Biomechanics, 39(6), 981-989.

Schmidt, H., Galbusera, F., Rohlmann, A., & Shirazi-Adl, A. (2013). What have we learned from finite element model studies of lumbar intervertebral discs in the past four decades?. Journal of biomechanics, 46(14), 2342-2355.

Schmidt, H., Kettler, A., Rohlmann, A., Claes, L., & Wilke, H. J. (2007a). The risk of disc prolapses with complex loading in different degrees of disc degeneration–a finite element analysis. Clinical Biomechanics, 22(9), 988-998.

Schmidt, H., Kettler, A., Heuer, F., Simon, U., Claes, L., & Wilke, H. J. (2007b). Intradiscal pressure, shear strain, and fiber strain in the intervertebral disc under combined loading. Spine, 32(7), 748-755

Schmidt, H., Heuer, F., Simon, U., Kettler, A., Rohlmann, A., Claes, L., & Wilke, H. J. (2006). Application of a new calibration method for a three-dimensional finite element model of a human lumbar annulus fibrosus. Clinical Biomechanics, 21(4), 337-344.

Shapiro, I., & Risbud, M. (2014). The intervertebral disc: Molecular and structural studies of the disc in health and disease

Sharma, M., Langrana, N. A., & Rodriguez, J. (1995). Role of ligaments and facets in lumbar spinal stability. Spine, 20(8), 887-900.

Shirazi-Adl, A. (2006). Analysis of large compression loads on lumbar spine in flexion and in torsion using a novel wrapping element. Journal of biomechanics, 39(2), 267-275.

Shirazi-Adl, A. (1994). Biomechanics of the lumbar spine in sagittal/lateral moments. Spine, 19(21), 2407-2414.

Shiraz-Adl, A. (1989). Strain in Fibers of a Lumbar Disc: Analysis of the Role of Lifting in Producing Disc Prolapse. Spine, 14(1), 96-103.

Shirazi-Adl, A. A. A. S. S., Ahmed, A. M., & Shrivastava, S. C. (1986). Mechanical response of a lumbar motion segment in axial torque alone and combined with compression. Spine, 11(9), 914-927.

Shirazi-adl, S. A., Shrivastava, S. C., & Ahmed, A. M. (1984). Stress Analysis of the Lumbar Disc-Body Unit in Compression A Three-Dimensional Nonlinear Finite Element Study. Spine, 9(2), 120-134.

Smith, L. J., Nerurkar, N. L., Choi, K. S., Harfe, B. D., & Elliott, D. M. (2011). Degeneration and regeneration of the intervertebral disc: lessons from development. Disease models & mechanisms, 4(1), 31-41.

Soini, J., Antti-Poika, I., Tallroth, K., Konttinen, Y. T., Honkanen, V., & Santavirta, S. (1991). Disc degeneration and angular movement of the lumbar spine: comparative study using plain and flexion-extension radiography and discography. Clinical Spine Surgery, 4(2), 183-187.

Waters, T. R., Putz-Anderson, V., Garg, A., & Fine, L. J. (1993). Revised NIOSH equation for the design and evaluation of manual lifting tasks. Ergonomics, 36(7), 749-776.

Watkins, J. (2010). Structure and function of the musculoskeletal system. Human Kinetics 1.

White III, A.A., Panjabi, M.M.(1990). Clinical Biomechanics of the Spine, second ed. Lippincott Williams & Wilkins.